Chapter 3
Plant-Mediated Fabrication of Gold Nanoparticles and Their Applications

Azamal Husen, Qazi Inamur Rahman, Muhammad Iqbal, Mansur Osman Yassin, and Rakesh Kumar Bachheti

3.1 Introduction

Nanotechnology, dealing with tiny particles of 1–100 nm, has gained increasing attention over the last three decades. These particles are commonly used in the household, industrial, and healthcare products and also have enormous potential in the nanotechnology-driven smart agriculture (Boxi et al. 2016; Fraceto et al. 2016; Siddiqi et al. 2016, 2018a, b, c, d; Siddiqi and Husen 2016, 2017a, b; Ovais et al. 2017). At present, above 1000 commercial products containing nanoparticles (NPs) are available in the market (Vance et al. 2015). The main challenges encountered during the fabrication of NPs relate to creating the desired shape, size, and monodispersity; and hence a refinement in the fabrication process is consistently required.

In general, NPs are fabricated by using two modes of preparation, i.e., the "bottom-up" (buildup of a material from the bottom: atom by atom, molecule by molecule, or cluster by cluster) and "top-down" (slicing or successive cutting of a bulk

A. Husen (✉)
Department of Biology, College of Natural and Computational Sciences, University of Gondar, Gondar, Ethiopia

Q. I. Rahman
Department of Chemistry, College of Natural and Computational Sciences, University of Gondar, Gondar, Ethiopia

M. Iqbal
Department of Botany, Faculty of Science, Jamia Hamdard (Deemed University), New Delhi, India

M. O. Yassin
Department of Surgery, College of Medicine and Health Sciences, University of Gondar, Gondar, Ethiopia

R. K. Bachheti
Department of Industrial Chemistry, Addis Ababa Science and Technology University, Addis Ababa, Ethiopia

A. Husen, M. Iqbal (eds.), *Nanomaterials and Plant Potential*,
https://doi.org/10.1007/978-3-030-05569-1_3

material to get nano-sized particle) procedures (Husen and Siddiqi 2014). The "bottom-up" procedure is usually preferred in both the chemical and biological syntheses of NPs (Vijayaraghavan and Nalini 2010; Narayanan and Sakthivel 2010a). On the other hand, the "top-down" procedure usually works with the material in bulk form, and the size reduction to the nanoscale is then achieved by specialized ablations, for instance, thermal decomposition, mechanical grinding, etching, cutting, lithography, laser ablation, and sputtering. The main demerit of this procedure is the surface structural defects, which have a significant impact on the physical features and surface chemistry of the metallic NPs.

Synthesis of metallic NPs through chemical reduction of metal salts in solution phase is most common (Lin et al. 2010), while physical approaches to synthesize metallic NPs include ultraviolet irradiation (Kundu et al. 2007), laser ablation (Tsuji et al. 2003), radiolysis (Meyre et al. 2008), sonochemistry (Okitsu et al. 2007), and so forth. Both the chemical and physical methods have been successful in producing well-defined NPs, but the use of plants or herbal extracts in NP fabrication has emerged as an alternative approach during the last few decades. This methodology is simple, cost-effective, and eco-friendly and can be easily scaled up for high yields (Husen and Siddiqi 2014, 2017a; Husen 2017). The extraction is done by soaking of plant samples in a green solvent; the extract so obtained contains flavonoids, terpenoids, proteins, reducing sugars, alkaloids, and other metabolites that act as the reducing and capping agents for reducing the metallic ions, and their concentrations are critical in governing the particle shape. The dried plants and their parts can be stored for longer time at room temperature, while fresh samples should be preserved at –20 °C to avoid deterioration. Moreover, since the seasonal and ontogenetic variations in phytochemical constituents are very common (Iqbal et al. 2011, 2018), dried plant samples collected at a proper time can be stored and used when needed. Thus, biogenic fabrication of NPs can occur with living as well as inactivated plant biomasses. Gardea-Torresdey et al. (2002, 2003) reported the possibility of using live alfalfa plants for the bioreduction of Au(III) to Au(0), which produced gold NPs ranging in size from 6 to 10 nm. *Brassica juncea* and *Medicago sativa* were also used to produce gold NPs at room temperature (Bali and Harris 2010). Aqueous extracts obtained from several plant leaves, roots, bark, seeds, fruits, galls, and petals have been used for this purpose (Table 3.1). Certain parameters such as pH, concentration, and temperature of reaction mixtures have to be adjusted to obtain certain size range, shape, and stability of the particles (Husen 2017; Siddiqi and Husen 2017a).

Gold NPs have drawn greater attention in the recent years due to their widespread uses. They have a larger surface area, higher dispersion owing to their very small size, and are highly stable and biocompatible. Some recent studies have elucidated the plausible positive and negative effects of gold NPs on plant growth and development (Siddiqi and Husen 2016). This chapter presents an overview of (a) the recent techniques of plant-mediated fabrication of gold NPs; (b) their characterization by UV-vis spectroscopy, thermogravimetric analysis, X-ray diffractometry, and SEM/TEM, among others; and (c) their application in some cutting-edge areas.

Table 3.1 Plant-mediated synthesis of gold nanoparticles, characterization techniques employed, and their application

Botanical name	Plant part used	Solvent used	Synthesis condition	Characterization techniques	Shape and Size	Phytoconstituents responsible for reduction of gold ion	Application	References
Abelmoschus esculentus	Pulp	Distilled water	Extract mixed with ingredient; reaction at room temperature with continuous stirring for 6 h	XRD, UV-vis, FTIR, RTEM, EDX, DLS	Spherical, triangle, and hexagonal; 4–32 nm	Phytochemicals, viz., vitamins and proteins	Anticancer and antimicrobial	Mollick et al. (2014)
Acacia nilotica	Leaf	Distilled water	Room temperature and mild condition	HRTEM, EDX, FTIR, XRD	Spherical; 6–12 nm	Flavonoids, tannins, triterpenoids, saponin, and polyphenolic compounds	Photocatalysis	Majumdar et al. (2013)
Aegle marmelos	Leaf	Distilled water	Solution based; mixing of ingredients; color change	UV-vis, XRD, FTIR, TEM, EDX, SAED, zeta potential	Mostly spherical; few irregular; 10.5–38 nm	Extract rich in polyphenolic tannin molecules	Detection of vitamin B or thiamine	Rao and Paria (2014)
Aloe vera	Leaf	Distilled water	Solution based; mixing of ingredients; reaction set for completion	UV-vis, XRD, FTIR, FESEM, EDX, HRTEM, SAED	Spherical and triangular; ~ 350 nm	Carbonyl, alcohols, phenols, and carboxylic acid derivative	–	Chandran et al. (2006)
Amomum subulatum	Black cardamom extract	Distilled water	Solution based; mixing of ingredients; reaction at appropriate pH; change in the solution color	UV-vis, XRD, FTIR, TEM, EDX	Different shapes and sizes; varying ratio of $AuCl_4$ ions/ plant extract	1,8-cineole, β-pinene, and α-terpineol	–	Singh and Srivastava (2015)
Andrographis paniculata	Leaf	Distilled water	Solution based; sonication	UV-vis, XRD, FESEM, FTIR, EDX, HRTEM, SAED	Spherical; 5–75 nm	Phenolic acids, antioxidants, and flavonoids	Anticancner	Babu et al. (2012)
Antigonon leptopus	Leaf	Distilled water	Solution based; mixing of ingredients; reaction set at particular pH	UV-vis, XRD, FTIR, HRTEM, EDX, SAED, DLS	Spherical; 13–28 nm	Carbonyl, amide, and carboxylic groups	Antioxidant and anticancer	Balasubramani et al. (2015)
Artemisia capillaris	*A. capillaris* water extract	Distilled water	Solution based and used sonication	UV-vis, FTIR, XRD, TEM	Spherical; 17–29 nm	Flavonoids, amino acid, and phenolic compounds	Catalyst activity	Lim et al. (2016)
Beta vulgaris	Pulp	Distilled water	Solution based; mixing of ingredients; fixed at appropriate pH	UV-vis, FTIR, EDX, HRTEM, SAED	Nanowires: shape and size vary with extract concentration and pH	Protein and polysaccharides	–	Castro et al. (2011)

(continued)

Table 3.1 (continued)

Botanical name	Plant part used	Solvent used	Synthesis condition	Characterization techniques	Shape and Size	Phytoconstituents responsible for reduction of gold ion	Application	References
Cacumen platycladi	Leaf	Distilled water	Solution based; mixing of ingredients; reaction set at water bath at particular pH	UV-vis, XRD, FTIR, HRTEM, EDX, SAED, TG	Spheres, triangles, and hexahedrons; changes with respect to pH	Flavonoid and reducing sugar	–	Zhan et al. (2011)
Camellia sinensis	Leaf	Distilled water	Solution based; mixing of ingredients; the change in the color	UV-vis, FTIR, HRTEM, CV	Nanorods and nanoprisms; mean diameter ~ 20 nm	Polyphenolic compounds especially polyphenols and flavonoids	–	Begum et al. (2009)
Cassia tora	Leaf	Distilled water	Solution based mixing of ingredients	UV-vis, FTIR, HRTEM, DLS, zeta potential	Spherical; mean diam. ~ 5 nm	Amides, alcohols, and aromatic compounds	Anticancer and antioxidant	Abel et al. (2016)
Chenopodium album	Leaf	Distilled water	Solution method: change in color of solution	UV-vis, XRD, FTIR, EDX, TEM	Quasi-spherical; 10–30 nm	Oxalic acid	–	Dwivedi et al. (2010)
Cinnamomum zeylanicum	Leaf	Distilled water	Solution based; mixing of ingredients; change in the color of solution	UV-vis, XRD, FTIR, HRTEM, SAED, PL	Spherical; an average size 25 nm	Terpenoids like eugenol, cinnamaldehyde, tannin, and sucrose	Photoluminescence (PL)	Smitha et al. (2009)
Commelina nudiflora	Whole plants	Distilled water	Solution based; mixing of ingredients; change in color	UV-vis, XRD, FESEM, FTIR, EDX	Spherical; 50–150 nm	Polysaccharides (sugar) and proteins	Antibacterial and antioxidant	Kuppusamy et al. (2015)
Coriandrum sativum	Leaf	Distilled water	Solution based; mixing of ingredients; change of color of solution	UV-vis, XRD, FTIR, EDX, TEM, SAED	Spherical, triangles, and decahedral; 8–58 nm	Active biomolecules, viz., amine, amide, and carboxylic group in protein	–	Narayanan and Sakthivel (2008)
Cymbopogon flexuosus	Leaf	Distilled water; chloroform	Column chromatography	UV-vis, FTIR, TEM, AFM, SAED, NMR	Triangular; mean diameter ~80 nm	Ketones, aldehydes, and carboxylic acids	–	Shankar et al. (2004)
Cystoseira baccata	Leaf	Distilled water	Mixing of ingredients with leaf extract; solution kept under stirring for 24 h	UV-vis, XRD, FTIR, HRTEM, EDS, STEM, zeta potential	Spherical; ~2.2 ± 8.4 nm	Polysaccharides, phenolic compounds, proteins, vitamins, and terpenoids	Anticancer	González-Ballesteros et al. (2017)

Dillenia indica	Fruit	Distilled water	Solution based; mixing of ingredients; change in the color of solution	UV-vis, XRD, FTIR, HRTEM, TGA, DSC	Spherical, triangular, tetragonal, pentagonal; irregular contours; 5–50 nm	High phenolic content	Cytotoxicity study	Sett et al. (2016)
Diospyros kaki and *Magnolia kobus*	Leaf	Distilled water	Mixing of reactant and then reaction set for reflux at water bath, 25–95 °C	FTIR, ESEM, AFM, RTEM, XPS, EDX	A mixture of plate (triangles, pentagons, hexagons) and spheres; 5–300 nm	Some proteins, terpenoids having functional groups of amines, alcohols, ketones, aldehydes, and carboxylic acids	–	Song et al. (2009)
Euphorbia hirta	Leaf	Distilled water	Solution based; mixing of ingredients; reaction set for a week	UV-vis, XRD, FTIR, EDX, HRTEM, AFM, SAED, Raman	Spherical; 10–50 nm	Various biomolecules	Antibacterial	Annamalai et al. (2013)
Guggulutiktam kashayam	Herb	Distilled water	Solution method: change in color of solution	UV-vis, XRD, FTIR, EDX, TEM	Spherical; 20–35 nm	Several biomolecules	Catalytic activity	Suvith and Philip (2014)
Madhuca longifolia	Leaf	Distilled water	Mixing of ingredients; reaction at fixed pH 2, under continuous stirring	UV-vis, FTIR, TEM, fluorescence emission	Triangular nanoplates; 7 nm to 3 μm	Plant proteins, viz., tyrosine	IR blocker	Fayaz et al. (2011)
Momordica charantia	Fruit	Distilled water	Solution based; mixing of ingredients; set at 100 °C	UV-vis, XRD, FTIR, HRTEM, EDX, SAED	Spherical; 30–100 nm	Triterpenes, proteins, and steroids	Depletion of nitrate reductase activity	Panday et al. (2012)
Moringa oleifera	Flower	Distilled water	Solution based; mild condition	TEM, UV-vis, SEM, EDX, Zeta potential	Spherical; 3–6 nm	Trace aromatic but abundant aliphatic compounds, i.e., proteins and lipids	Catalytic reduction and anticancer	Anand et al. (2015)
Morinda citrifolia	Root	Distilled water	Solution based; mixing of ingredients; changes in color of solution	UV-vis, XRD, FTIR, FESEM, EDX, HRTEM, AFM	Spherical and triangular; 12–38 nm	Protein associated with amide, carbonyl, aldehyde groups	–	Suman et al. (2014)
Musa paradisiaca	Peel	Distilled water	Solution based; mixing of ingredients; solution at 353 K for 20 min, change in solution color	UV-vis, XRD, FTIR, SEM, EDX, TEM, zeta potential	Spherical and triangular; ~ 50 nm	Phenols and carboxylic acids and amide compounds	Antibiotic resistance and anticancer	Vijayakumar et al. (2017)

(continued)

Table 3.1 (continued)

Botanical name	Plant part used	Solvent used	Synthesis condition	Characterization techniques	Shape and Size	Phytoconstituents responsible for reduction of gold ion	Application	References
Naregamia alata	Leaf	Distilled water	Mixing of ingredients with leaf extract; solution put in the microwave reactor for 1mint	UV-vis, XRD, FTIR, FESEM, EDX, HRTEM, AFM	Polyshaped nanoparticles; ~9.19 ± 27.92 nm	Secondary flavonoids	Catalysis	Francis et al. (2017b)
Nigella sativa	Seeds	Distilled water	Seed extract in water by soaking and boiling and mixed with ingredient change in color of solution	TEM, UV-vis, FTIR, EDX	Spherical, triangular, and hexagonal; 15–29 nm	Vapors rich in amide, alcohol, phenolic group compounds, and their derivatives	Antibacterial and anticancer	Manju et al. (2016)
Olea europaea	Leaf	Distilled water	Solution method: mixing of reactant at appropriate pH; change in color of solution	UV-vis, FTIR, XRD, TEM, TGA	Triangular, hexagonal, and spherical; 50–100 nm	Potential biomolecules, viz., oleuropein, apigenin-7-glucoside, and/or luteolin-7-glucoside	–	Khalil et al. (2012)
Pistacia integerrima	Gall extract of *Pistacia integerrima*	Distilled water	Solution based; mixing of ingredients; color change at particular pH	UV-vis, XRD, FTIR, SEM, EDX, TEM	Spherical; shapes changing with pH change; 20–200 nm	Terpenoids having functional groups of amines, alcohol, phenol, aldehyde, ketones, and carboxylic acid	Enzyme inhibition, antibacterial, antifungal, antinociceptive, muscle relaxant, and sedative	Islam et al. (2015a, b)
Plumbago zeylanica	Bark	Distilled water	Solution based; mixing of ingredients with bark extract; change in color of solution	UV-vis, XRD, FTIR, SEM, TEM, EDX	Spherical; ~ 28 nm	Plumbagin and hydroplumbagin glucoside containing many hydroxyl groups	Antioxidant, antimicrobial, and cytotoxic	Velammal et al. (2016)
Punica granatum	Juice	Distilled water	Solution based; after mixing ingredients set the reaction for 24 h; change in color	UV-vis, XRD, FTIR, HRTEM, SAED	Spherical, triangular, and hexagonal; 23–35 nm	Terpenoids, alkaloids, sugar, amino acid, polyphenols, fatty acids, aromatic compounds	Catalytic reduction	Dash and Bag (2014)
Rosa hybrid	Petal	Distilled water	Solution based; mixing of ingredients; reaction set on magnetic heater stirrer at 80 °C for 1 h	UV-vis, XRD, FTIR, EDX, XPS, HRTEM, SAED, DLS	Polydispersed spherical, triangular, and hexagonal; ~10 nm	Sugar and proteins	–	Noruzi et al. (2011)

Salicornia brachiata	Extract	Distilled water	Solution based; mixing of ingredients; solution at 60 °C with trace amount of $NaBH_4$, change in color of solution	UV-vis, XRD, FTIR, FESEM, EDX, HRTEM, SAED	Polydispersed spherical; 22–35 nm	Polyphenols, glycosides, flavonoids, carbohydrates, and protein	Catalytic and antibacterial	Ahmad et al. (2014)
Salix alba	Leaf	Distilled water	Solution based; reactant-mixed; color change recorded	UV-vis, FTIR, SEM, AFM	Spherical; 50–80 nm	Amines, amide, and aromatic groups	Enzyme inhibition, antibacterial, antifungal, antinociceptive, muscle relaxant and sedative	Islam et al. (2015)
Sapindus mukorossi	Pericarp (soap nut shells)	Distilled water	Solution method: change in color of solution	UV-vis, FTIR, XRD, TEM, EDX, SAED	Quasi-sphere; 6–15 nm	Carboxylic groups in the saponins and the carbonyl groups in the flavonoids	Catalytic activity	Reddy et al. (2012)
Sphaeranthus amaranthoides	Leaf	Distilled water	Solution based: mixing of ingredients; change in the color	UV-vis, FTIR, EDX, HRTEM	Spherical; 39–47 nm	Carbohydrate, tannins, saponins, steroids, glycosides, terpenoids, and alkaloids	–	Nellore et al. (2012)
Stevia rebaudiana	Leaf	Distilled water	Solution based; mixing of ingredients; set at a rotation rate of 150 rpm at 30 °C	UV-vis, XRD, FTIR, HRTEM, EDX, SAED, TG	Octahedral and some nanohexagons; 8–20 nm	Phytochemical present in extract	–	Mishra et al. (2010)
Stevia rebaudiana	Leaf	Distilled water	Solution based; mixing of ingredients; set for reaction with continuous stirring	UV-vis, XRD, FTIR, SEM, EDX, TEM, Zeta Potential	Spherical, 5–20 nm	Terpenoids and proteins	–	Sadeghi et al. (2015)
Terminalia catappa	Leaf	Distilled water	Solution method, mixing of reactant; changes in the color of solution	UV-vis, XRD, FTIR, TEM	Spherical; 10–35 nm	Hydrolysable tannin, polyphenols and carboxylic compounds	–	Ankamwar (2010)
Terminalia arjuna	Fruit extract	Distilled water	Solution based: mixing of ingredients; change in the color of solution	UV-vis, XRD, FTIR, TEM, EDX, SAED, AFM, DLS, zeta potential	Spherical; 5–50 nm	Tannin, terpenoid, saponins, flavonoids, glycosides, and polyphenolic compounds	Seed germination enhancer	Gopinath et al. (2014)

(continued)

Table 3.1 (continued)

Botanical name	Plant part used	Solvent used	Synthesis condition	Characterization techniques	Shape and Size	Phytoconstituents responsible for reduction of gold ion	Application	References
Terminalia arjuna	Leaf	Distilled water	Solution based; mixing of ingredients; change the color of solution	UV-vis, XRD, FTIR, SEM, TEM, EDX, AFM, SAED	Spherical; 20–50 nm	Arjunetin, leucoanthocyanidins, and hydrolyzable tannins	Induces mitotic cell division and pollen germination	Gopinath et al. (2013)
Terminalia arjuna	Bark	Distilled water	Aliquot of bark extract mixed with reactant; solution fixed at 80 °C for 15 min; change in the solution color	UV-vis, XRD, FTIR, FESEM, HRTEM, EDX, DLS, zeta potential	Spherical and triangular; 20–50 nm	Polyphenols	Neuroprotective potential via antioxidant, anticholinesterase, and antiamyloidogenic effects	Suganthy et al. (2018)
Withania somnifera	Leaf	Distilled water; ethanol	Solution based; mixing of reactant; the reaction set at particular pH	UV-vis, FTIR, TEM, EDX	Spherical and hexagonal	The phenolic groups (–OH) residue	–	Bindhani and Panigrahi (2014)

3.2 Fabrication and Characterization of Gold Nanoparticles

The principal biomolecules such as amines, amino acids, aldehydes, ketones, carboxylic acids, phenols, proteins, flavonoids, saponins, steroids, alkaloids, and tannins and different nutritional compounds present in plant parts and their extracts reduce the metal ion to NP (Fig. 3.1 and Table 3.1). Gold NPs show a distinct optical response usually ascribed to the localized surface plasmon resonance (SPR), i.e., the collective oscillation of electrons in the conduction band of gold NPs in resonance with a specific wavelength of incident light. The SPR of gold NPs results in a strong absorbance band in the visible region of 500–600 nm, which can be measured by UV-Vis spectroscopy, the first technique used to characterize gold NPs. In addition, several other techniques such as transmission electron microscopy, scanning electron microscopy, X-ray diffraction, Fourier transform infrared spectroscopy, atomic force microscopy, energy-dispersive X-ray spectroscopy, dynamic light scattering, zeta potential, surface-enhanced Raman spectroscopy, nuclear magnetic resonance spectroscopy, and others are also used.

3.2.1 Fabrication of Gold Nanoparticles

As the seasonal changes and phyto-developmental stages considerably affect the chemical constituents in plant tissues (Iqbal et al. 2011, 2018), it is advised to collect the relevant plant material at a proper time and optimal stage of plant development and store it in dried form. The dried plant materials can be stored for long durations at room temperature. However, to avoid any deterioration, the material may be preserved at –20 °C. The extracts of the whole plant or plant parts (leaves, stems, roots, bark, seeds, flowers, or floral parts) in appropriate solvents contain the capping and reducing agents that are required to reduce the metallic ions. These biomolecules actively participate in the bioreduction process. Shankar et al. (2003) obtained gold NPs from geranium (*Pelargonium graveolens*) leaf extract. This fabrication process, resulting in gold NPs of spherical, triangular, decahedral, and icosahedral shapes, was accomplished within 48 h. The presence of terpenoids in the extract was held responsible for the reduction of gold ions and the formation of gold NPs. In another study, Chandran et al. (2006) produced gold NPs from *Aloe vera* leaf extract and controlled their shape and size; these were triangular in shape and 50–350 nm in size. Both the shape and size were dependent on the leaf extract quantity. Low concentration of the leaf extract added to chloroauric acid ($HAuCl_4$) solution increased the production of triangular NPs. With a high concentration of leaf extract, the ratio of nanogold triangles to sphericals was reduced. It was proposed that the carbonyl functional groups found in the leaf extract were responsible for the reduction of gold ions and NP production.

With the advancement in the plant-mediated NP fabrication techniques, some researchers used sun-dried leaf powder dissolved in water at ambient temperature as

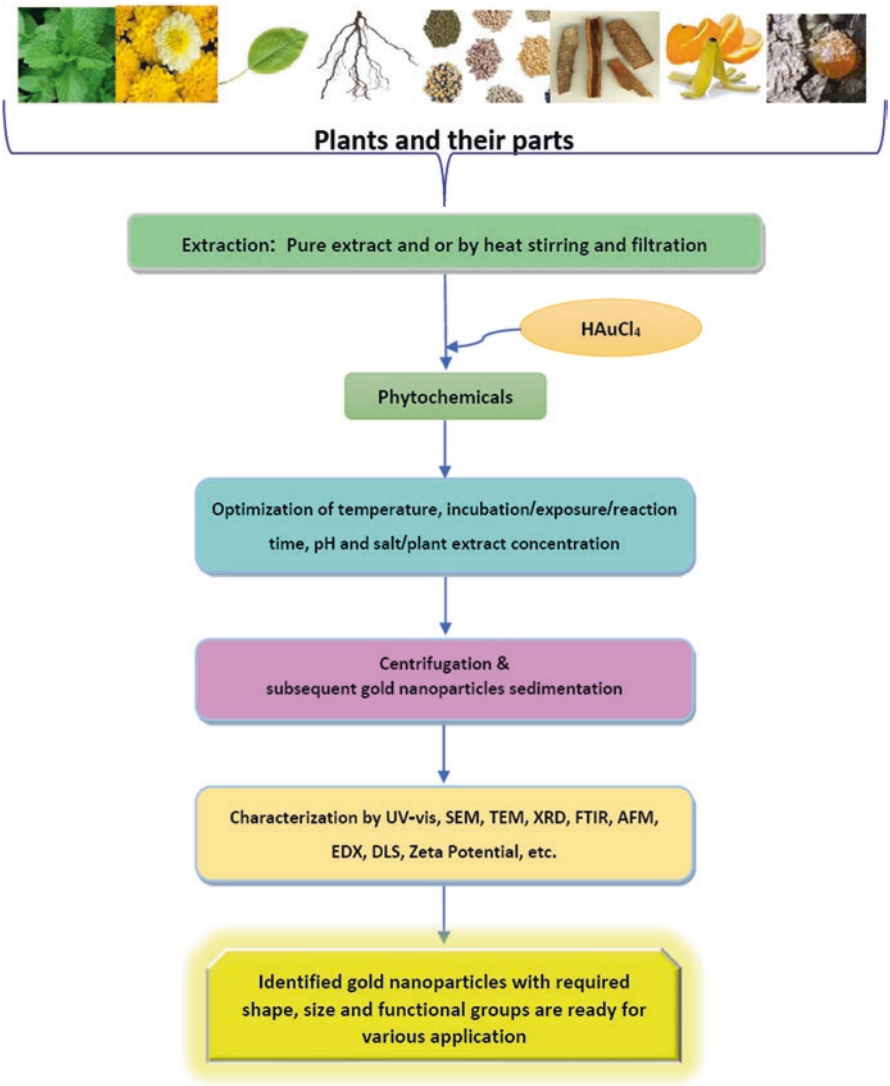

Fig. 3.1 Fabrication and characterization of gold nanoparticles using various plant parts

an alternative of the plant extract obtained by boiling. For this procedure, no accelerator/moderator, viz., ammonia, was required; nonetheless, the concentration of various plant leaf extracts was the rate-determining step. For instance, Huang et al. (2007a) used a sun-dried powder of *Cinnamomum camphora* leaves for the fabrication of gold and silver NPs at ambient temperature. They executed a series of experiments by adding 0.1 g and 0.5 g dried leaf extract to 50 mL of 1 mM aqueous $HAuCl_4$ and synthesized gold NPs of 100 nm and 200 nm size, respectively. Fourier transform infrared (FTIR) spectroscopy confirmed that the biomass of dried leaves

was rich in polyols, which were responsible for the bioreduction of Au^{3+} to Au^0. In another study, Phillip (2009) used the dried leaf powder extract of *Mangifera indica* for the synthesis of spherical gold NPs at room temperature. These particles were smaller, more uniform in size, and stable for more than 5 months. Further, FTIR spectroscopy has demonstrated the role of water-soluble compounds, such as flavonoids, terpenoids, and thiamine, as stabilizing agents in the gold NP fabrication.

Narayanan and Sakthivel (2010b) obtained gold NPs by using the aqueous extract of *Coleus amboinicus* leaves. The extract was rich in aromatic amines, amide (II) groups, and secondary alcohols, which acted as capping agent during the bioreduction of Au(III) to Au(0). Bioreduction of $HAuCl_4$ was successfully observed by monitoring the change in color of the solution by gradual addition of leaf extract; a distinct UV-vis absorption peak was seen at 536 nm, which corresponded to the SPR of gold NPs. The particles of different shapes (spherical, triangular, truncated triangular, hexagonal, and decahedral) measured 4.6–55.1 nm. Noruzi et al. (2011) described an inexpensive and easy method for facile synthesis of gold NPs from rose petals extract and $HAuCl_4$. With a 10% extract solution, 2 mM Au^{3+} solution failed to form gold NPs; on increasing the extract concentration, however, anisotropic gold NPs were successfully formed, which was confirmed by the peak at 750 nm in SPR spectrum. As the desired concentration of the extract is mixed with the Au^{3+} solution, the solution color changed from yellow (extract color) to violet within 5 min at room temperature, which indicated the formation of gold NPs. The SPR band at ≈525 nm confirmed the formation of gold NPs, which were polydispersed with different shapes (viz., spherical, triangular, and hexagonal) and an average particle size of 10 nm, as determined by the dynamic light-scattering (DLS) method. Philip et al. (2011) proposed an easy and cost-effective protocol based on the leaf extract of *Murraya koenigii* and $HAuCl_4$ solution. The leaf extract was reportedly rich in polyphenols, alkaloids, carbazole, and flavonoids, which were responsible for bioreduction of Au(III) into Au(0). The NPs produced were spherical, with an average size of 20 nm. These were quite stable, showing no aggregation for more than 2 months.

Nellore et al. (2012) reported a simple procedure to synthesize gold NPs by gradual addition of the leaf extract of *Sphaeranthus amaranthoides* into the $HAuCl_4$ solution, which changed the solution color from pale yellow to purple-red within 5 min, indicating the formation of NPs that exhibited a well-resolved SPR band at 525 nm. The SPR spectrum remained unchanged even after 30 days, indicating that the NPs produced were quite stable in aqueous solution without aggregation. FTIR spectroscopy of the leaf extract before and after the addition of gold solution revealed an abundance of carbohydrate, tannins, steroids, glycosides, terpenoids, and alkaloids in the leaf extract. High-resolution transmission electron microscopy (*HRTEM*) images confirmed that the synthesized NPs were polydispersed and predominantly spherical in shape with a size range of 39–47 nm. Ghosh et al. (2012) used flower extract (*Gnidia glauca*) for gold NP fabrication, which was evident by the change in color from yellow to dark-red in the visible range of the spectrum (450–600 nm). The reaction started 2 min after the interaction of flower extract with $HAuCl_4$ solution and was accomplished in 20 min, thus showing a greater efficiency in comparison to the earlier work of Vankar and Bajpai (2010), wherein the reaction

completed in ~2 h. Gopinath et al. (2013) synthesized spherical gold NPs of 20–50 nm by using the leaf extract of *Terminalia arjuna* with $HAuCl_4$ solution, whereas Annamalai et al. (2013) used *Euphorbia hirta* leaf extract and $HAuCl_4$ solution to obtain the monodispersed, almost spherical NPs of 10–50 nm. Majumdar et al. (2013) used $HAuCl_4$ salt solution with *Acacia nilotica* leaf extract rich in flavonoids, tannins, triterpenoids, and saponins, which facilitated the reduction of auric salt to neutral metal ions. The reaction resulted in highly crystalline monodispersed spherical gold NPs of 6–12 nm size. The particle size significantly decreased as the leaf extract concentrations were increased. Dash and Bag (2014) used *Punica granatum*juice, rich in phytochemicals (viz., terpenoids, sugar, polyphenols, alkaloids, fatty acids, and aromatic compounds) for fabrication of gold NPs, which were triangular, pentagonal, hexagonal, and spherical in shape. With 1440–2400 mg L^{-1} concentration of the juice extract, the average particle size exhibited a gradual decrease from 35.8 to 23.1 nm.

With progress in the plant-mediated fabrication of gold NPs, some researchers started using microwave radiation for rapid and easy NP synthesis. For instance, Yasmin et al. (2014) could fabricate the stable spherical gold NPs of 16–30 nm from the fresh chopped leaves of *Hibiscus rosa-sinensis* by using microwave heating for 3 min. The authors suggested that alkaloids and flavonoids present in the leaf tissue played a key role in the fabrication process. Likewise, Joseph and Mathew (2015a) used microwave radiation for this purpose using the extract of chopped fresh leaves of *Aerva lanata* boiled in distilled water. The extract was rich in various alkaloids, flavonoids, and other phytochemicals which brought about bioreduction of Au^{3+} to Au^0. The synthesized NPs were polydispersed and mostly spherical in general, with some being triangular, hexagonal, and plate-like in shape. The average diameter of spherical particles was 17.97 nm, exhibiting the characteristic SPR band at ~535 nm.

Stable gold NPs (triangular, hexagonal, and nearly spherical) were also fabricated by using 1 M $HAuCl_4$ and flower extract of *Moringa oleifera* (Anand et al. 2015). Free from impurity, these NPs of 5 nm average diameter were homogeneously distributed throughout and displayed a well-resolved SPR band at 540 nm. The ^{1}H-NMR spectroscopy and FTIR studies have confirmed that the secondary metabolites, viz., trace, aromatic but abundant aliphatic compounds (proteins and lipids), were involved in the bioreduction of $Au^{3+} \rightarrow Au^0$. Manju et al. (2016) made use of the *Nigella sativa* seed oil for this purpose. The NPs (spherical, triangle, and hexagonal) were in the range of 15–28.4 nm and showed a distinct SPR band at 540 nm.

In a recent study, Vijayakumar et al. (2017) have fabricated gold NPs using the extract of banana (*Musa paradisiaca*) peels and $HAuCl_4$ solution. Banana peel contains antioxidant compounds, viz., gallocatechin and dopamine, that caused bioreduction of Au(III) to Au(0). The triangular to spherical NPs of about 50 nm exhibited well-resolved SPR band at 541 nm which was characteristic of gold NPs. Suganthy et al. (2018) synthesized gold NPs by using bark extract of *Terminalia arjuna*. The phytochemicals present in the bark extract, including polyphenols such as (+)-catechin, ellagic acid, gallic acid, and their derivatives, were responsible to facilitate the reduction of Au^{3+} ions. The authors also succeeded in obtaining Au and Pd bimetallic NPs of different shapes. The gold NPs were anisotropic ranging in size

from 3 to 70 nm with average diameter of 30 nm and showing a broad SPR band near 536 nm. In another study, Raouf et al. (2017) used the dried powder as well as ethanolic extract of a red alga (*Galaxaura elongata*) to synthesize gold NPs. A strong SPR band was seen at ~535 nm and ~536 nm for the NPs formed by the algal ethanolic extract and the algal powder, respectively. The FTIR study showed a high percentage of andrographolide and alloaromadendrene oxides and suggested for the reduction of $HAuCl^{-}$, which acted as the stabilizing agent during synthesis. The particles were spherical in shape along with a few rods, triangular, truncated triangular, and hexagonal ones, and exhibited a wide range of size from 3.85 to 77.13 nm, which was inconsistent with zeta potential results.

3.2.2 Characterization of Gold Nanoparticles

The fabricated gold NPs exhibited distinct optical and physical properties, depending on their size (diameter), shape, surface structure, and agglomeration state. The various characterization techniques are summarized in Table 3.1.

3.2.2.1 Ultraviolet-Visible (UV-Vis) Spectroscopy

UV-vis spectroscopy is the most important analytical technique to characterize the formation and stability of gold NPs. The formation is determined by monitoring the change in color during the synthesis. When the reactant is mixed with appropriate plant extract (e.g., leaf, seed, flower, fruit, etc.), the color of the mixture changes (from yellow to violet) immediately. This is attributed to electromagnetic radiation with free electron present in the conduction band of gold NPs and exhibits strong absorbance band in the visible region (500–600 nm) known as SPR. Figure 3.2

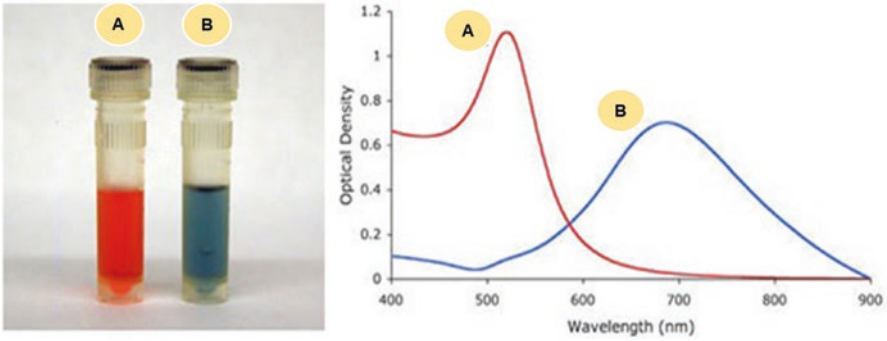

Fig. 3.2 Shape-dependent localized SPR as indicated by the visual appearance and UV-vis spectra of (**a**) the spherical and (**b**) urchin-shaped gold nanoparticles. (Adopted from: www.cytodiagnostics.com)

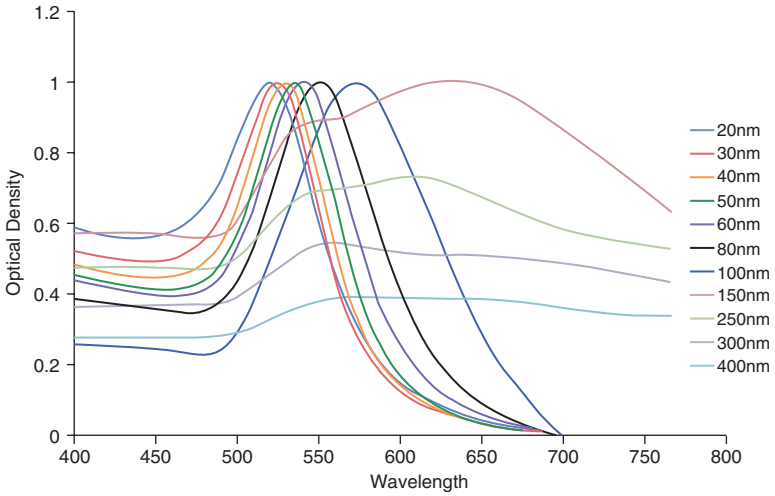

Fig. 3.3 Size-dependent SPR spectrum of gold nanoparticles, showing the presence of red shift of the absorption maximum, as the size of nanoparticles increases. (Adopted from: www.cytodiagnostics.com)

shows the shape-dependent SPR spectrum of gold NPs. As the particle diameter increases, absorption peak shifts toward higher wavelength. For uneven shaped particles such as gold nano-urchins, the absorption peak position shifts into the far red region of the spectrum as compared to the spherical particle of the same diameter. Figure 3.3 also reveals UV-vis spectra of gold NPs as a function of reaction time; it has been observed that there is no significant difference between the intensity of SPR bands in minutes 0, 5, 10, 15, 20, and 25, indicating that the reaction has been completed during the first minute.

The stability of synthesized gold NPs is strictly dependent on the degree of aggregation, i.e., irreversible interparticle coupling, which is accompanied by shifting of the characteristic absorption peak toward the red region of the electromagnetic radiation. Mollick et al. (2014) found the solution color changing from red to blue/purple while synthesizing gold NPs by using the *Abelmoschus esculentus* pulp extract stored at room temperature for 5 months. The UV-vis spectra (Fig. 3.4) produced the SPR band at 538 nm without any significant change in the absorbance intensity. The synthesized NPs were stable at room temperature for a long period of time.

3.2.2.2 Microscopy

Scanning electron microscopy (SEM), transmission electron microscopy (TEM), and atomic force microscopy (AFM) are used to study the morphological features of synthesized gold NPs effectively. SEM is used to examine the morphology of as-synthesized nanomaterials to determine the shapes of particles and their surface features at nanoscale level. It measures electron scattering from the surface of the sample, which requires highly accelerated short wavelength electrons for

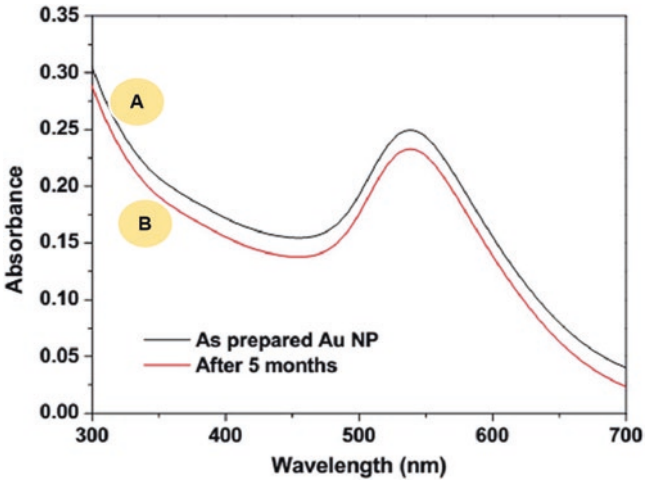

Fig. 3.4 UV-vis absorption spectra of gold nanoparticles synthesized by using pulp extract of *Abelmoschus esculentus*; (**a**) after reaction accomplished; (**b**) after 5 months at room temperature. (Adopted from: Mollick et al. 2014)

high-resolution images, which could be magnified up to 200,000 times. Chandran et al. (2014) successfully synthesized gold NPs by using leaf extracts of two medicinally important plants *Cucurbita pepo* and *Malva crispa* as shown in Fig. 3.5. The elemental and chemical compositions of as-synthesized gold nanomaterials are determined by energy-dispersive spectroscopy (EDS), which is usually attached with either FESEM or TEM. When the highly energetic electron beam is focused over the nanomaterial, each of its constituent elements emits characteristic energy X-rays by electron beam irradiation.

In the case of TEM, high-energy electrons accelerated with 200 KV are transmitted through an ultrathin specimen. After successful interaction with the sample, electrons are transmitted, and an image appears on the screen which provides information of the bulk material from very low to high magnification. TEM is typically used to determine the physical size of as-synthesized materials and their nature (crystalline or amorphous). Figure 3.6 includes TEM micrographs revealing different features of gold NPs synthesized by using the leaf extract of *Acacia nilotica* at 60 (Fig. 3.6a–e), 100 (Fig. 3.6f–g), and 200 mg L^{-1} (Fig. 3.6i–k) concentrations. The synthesized NPs were predominantly spherical in shape. As the concentration of the extract increased from 60 to 200 mg L^{-1}, the average particle size varied from 12.24 to 5.99 nm. Figure 3.6c shows HRTEM image of gold NPs with d-spacing value of 0.24 nm, which matched fully with the expected d-spacing of the [111] plane of face-centered cubic crystalline Au (JCPDS, no. 04–0784). Selected area electron diffraction (SAED) is a crystallographic experimental technique that can be linked to TEM in order to obtain valuable insight regarding the crystalline nature of the material synthesized and its analogy to X-ray powder diffraction. The SAED patterns can be used to identify the crystal structures and measure the lattice parameters. Figure 3.6h shows the SAED pattern obtained from a gold NP; the diffraction

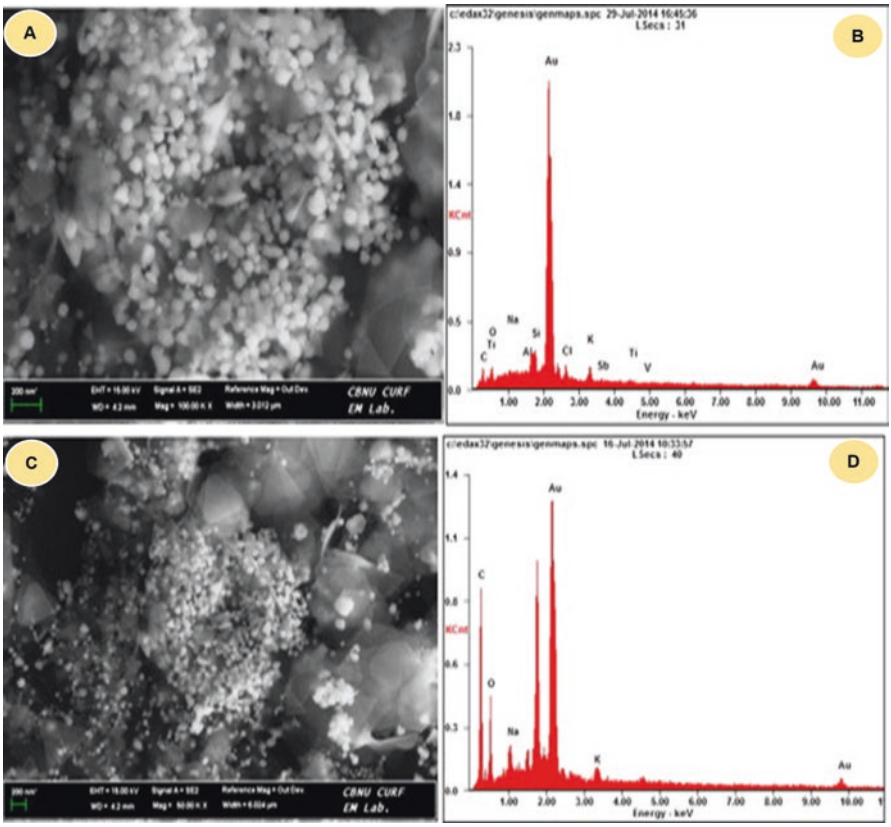

Fig. 3.5 FE-SEM image of gold nanoparticles synthesized from pumpkin leaf extract (**a**) and their EDS analysis (**b**); the FE-SEM image of gold NPs synthesized from curled mallow leaves (**c**) and their EDS analysis (**d**). (Adopted from: Chandran et al. 2014)

rings from inner to outer associated with [111], [200], [220], and [311] atomic planes of Au indicate the formation of crystalline gold NPs.

AFM analytical technique is effectively used to study the topology of a sample in three dimensions (x, y, and z). It can measure the height of sample which is not possible with FESEM. Gopinath et al. (2014) worked out the surface morphology of the as-synthesized gold NPs by AFM analysis as shown in Fig. 3.7. The micrograph reveals that the as-synthesized gold NPs possess spherical shape and are 20–50 nm in size.

3.2.2.3 X-Ray Diffraction (XRD)

This technique is used to analyze the crystal structure, phase, and other structural parameters such as average grain size, crystallinity, strain, and crystal defects. When X-ray interacts with crystalline phase of materials, it produces diffraction peaks.

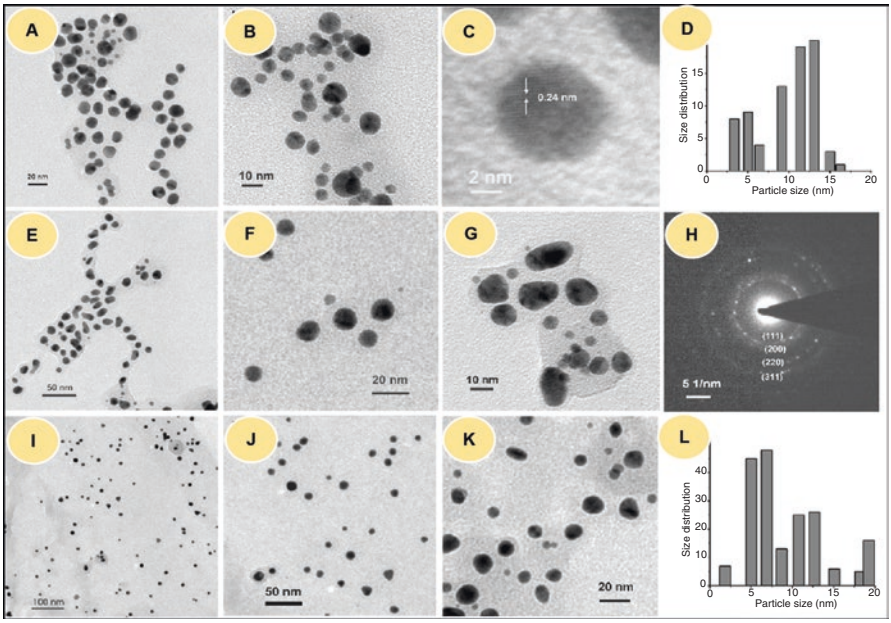

Fig. 3.6 TEM images, SAED, and histograms showing the effect of the concentration of leaf extract of *Acacia nilotica* on the size of gold nanoparticles: (**a**–**e**) of gold nanoparticles at 60 mgL^{-1}, TEM images (**f**–**g**) of gold nanoparticles at 100 mgL^{-1}, TEM images (**i**–**k**) of nanoparticles at 200 mgL^{-1}, (**h**) SAED of gold nanoparticle, and (**d**, **l**) histograms of gold nanoparticles at 60 and 200 mgL^{-1}, respectively. (Adopted from: Majumdar et al. 2013)

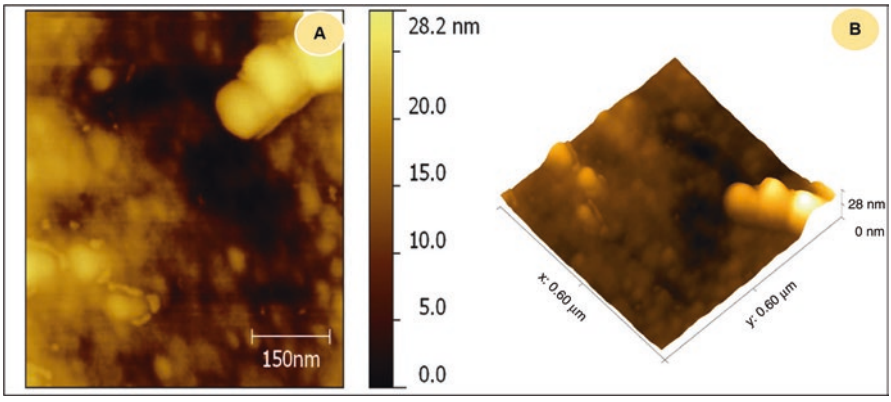

Fig. 3.7 AFM image of gold nanoparticles using aqueous fruit extract of *Terminalia arjuna*: (**a**) 2D image and (**b**) 3D image. (Adopted from: Gopinath et al. 2014)

The intensity of peaks reflects the distribution of atoms within the lattice, and these peaks can be used as "fingerprints" for identification of solid phases. Figure 3.8a shows a diffractogram of gold NPs synthesized by using *Terminalia arjuna* fruit; major reflections appear at 38.24°, 44.45°, and 66.30° corresponding to (111),

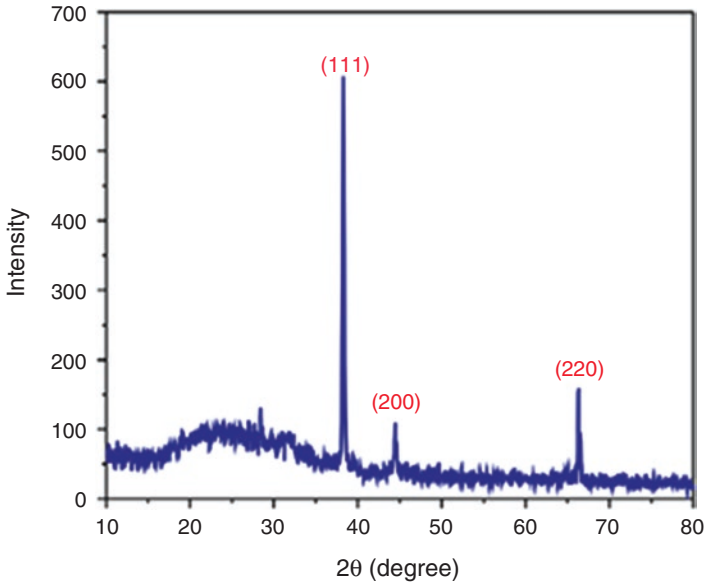

Fig. 3.8 XRD pattern of gold nanoparticles synthesized by using fruit extract of *T. arjuna* with $HAuCl_4$ aqueous solution. (Adopted from: Gopinath et al. 2014)

(200), and (220) planes, which confirm that these NPs belong to face-centered cubic phase of gold, as per the JCPDS card no. 04–0784 and the Au° nature of NPs (Gopinath et al. 2014). Singh and Srivastava (2015) reported that pH plays an important role in the synthesis of gold nanomaterials and that different morphologies of Au NMs can be observed by changing the pH conditions. Figure 3.8b shows that there is no change in d-spacing value, as all similar planes in XRD peaks correspond to the same 2θ value. Suman et al. (2014) effectively calculated the mean size of gold NPs (synthesized from the root extract of *Morinda citrifolia*) by using the Debye-Scherrer equation to determine the width of (111) Bragg's reflection, which was around 15 nm.

3.2.2.4 Dynamic Light Scattering (DLS) and Zeta Potential Analysis

DLS provides important information regarding the size of as-synthesized NPs and their distribution. It involves illumination of a particle suspension by laser beam, which results in temporal fluctuation of the elastic scattering intensity of light, i.e., Rayleigh scattering4125 induced from the Brownian motion of the particles of a size much smaller than the incident light wavelength, at a fixed scattering angle. Gopinath et al. (2014) reported the size of gold NPs in the range 5–60 nm with an average of 25 nm; however, the size of some particles increased due to agglomeration as revealed in Fig. 3.9a showing the DLS result. Zeta potential is a physical property, which is used to analyze the stability of synthesized NPs; it measures the

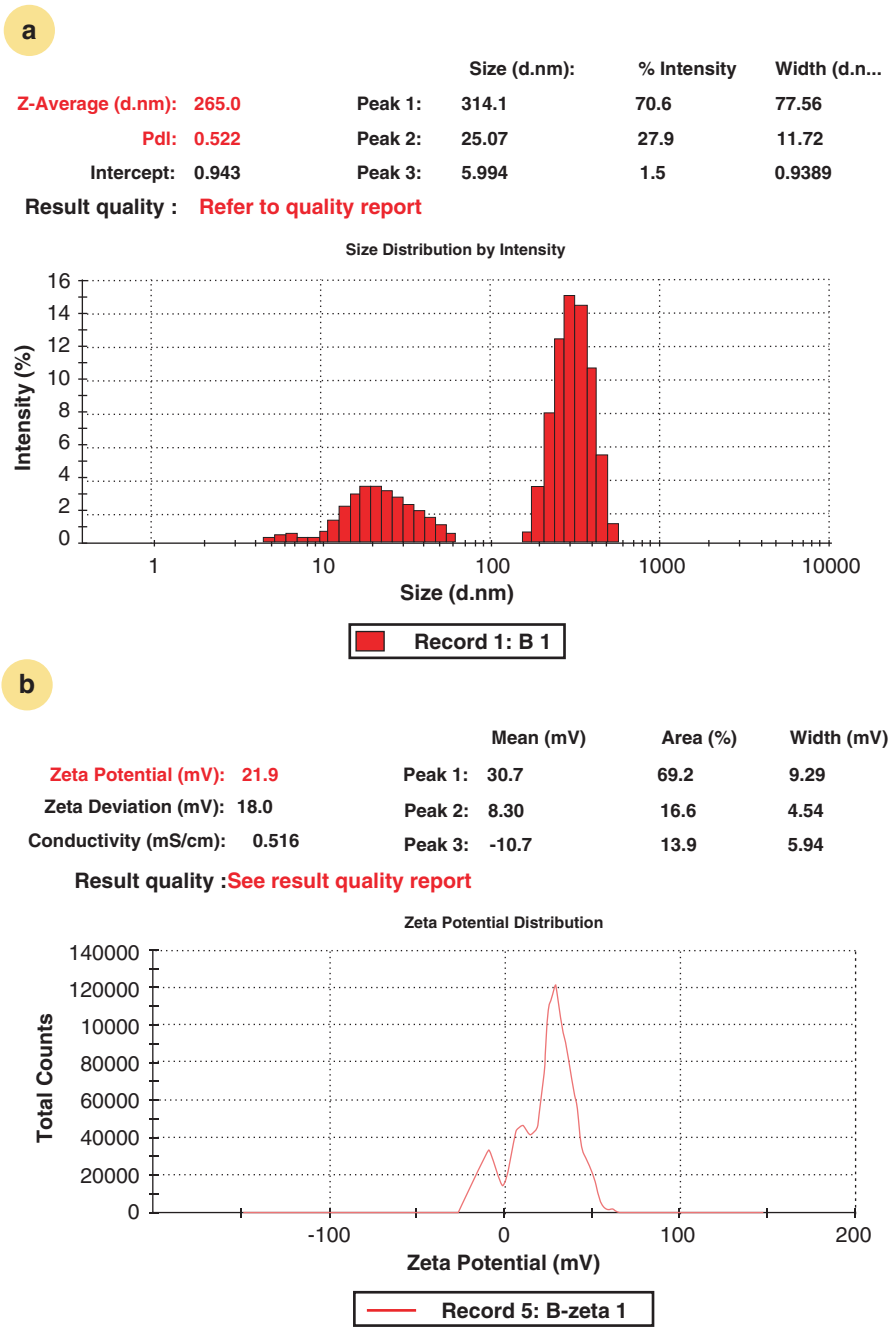

Fig. 3.9 (**a**) Particle size distribution of gold nanoparticles synthesized with the assistance of *Terminalia arjuna* fruit extract through the DLS method; (**b**) measurement of zeta potential analysis to determine the stability of these particles. (Adopted from: Gopinath et al. 2014)

potential difference between two suspended particles present in the colloidal suspension. Its value may be positive or negative ranging between –30 mV and + 30 mV. Figure 3.9b shows the zeta potential measurement of synthesized gold NPs having a value of 21.9 mV, which means that the surface of the NPs has a net positive charge.

3.2.2.5 Fourier Transform Infrared Spectroscopy (FTIR)

FTIR spectroscopy is used to examine the purity and composition of synthesized NPs. It measures the interaction of infrared radiation with molecules. In the green route of NP synthesis, biomolecules of secondary metabolites are responsible for reducing gold ions and acting as capping agents for the facile synthesis of gold NPs. Geetha et al. (2013) successfully synthesized gold NPs by using *Couroupita guianensis* extract and $HAuCl_4$ solution. Interpretation of FTIR spectra reveals the biomolecules responsible for the reduction of gold ions and capping of the bioreduced AuNPs, as shown in Fig. 3.10; the intense broad absorption at 3414 cm^{-1} is the characteristic peak for hydroxyl functional group in phenols and alcoholic compounds. A comparison of the gold NP spectrum, a and b, indicates correlation between the peak and the –OH in the –COOH group; the peak appeared at 3414 cm^{-1} in raw material, but it was narrower and shifted to longer wave number 3615 cm^{-1} after encapsulation of NPs. The peaks at 1073, 1288, 1383, and 1648 cm^{-1} are reduced, and a new peak appeared at 1744 cm^{-1} which indicates that the alcoholic group is converted into aldehyde to reduce Au^{3+} to Au^0. Similarly, Jayaseelan et al. (2013) reported the FTIR pattern of the gold NPs obtained with the aqueous seed

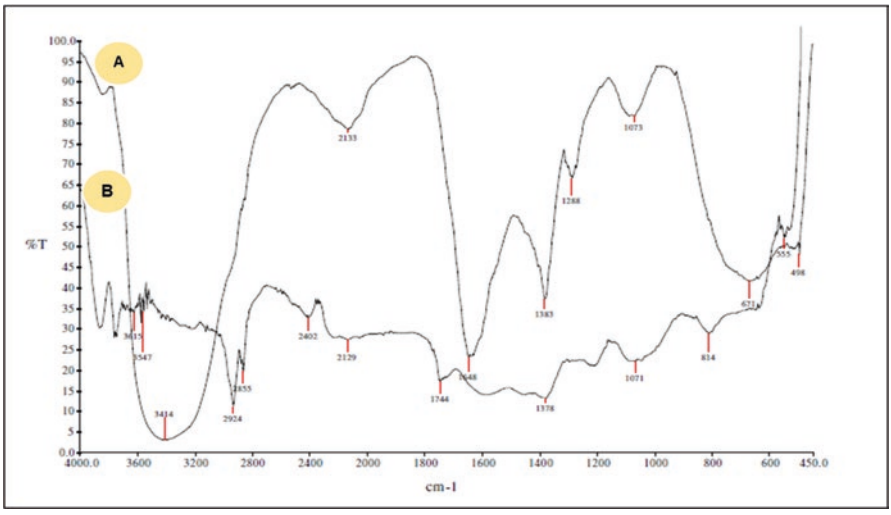

Fig. 3.10 FTIR spectra: (**a**) flower extract of *Couroupita guianensis*, (**b**) gold nanoparticles synthesized by *C. guianensis* flower extract. (Adopted from: Geetha et al. 2013)

extract of *Abelmoschus esculentus* exhibiting bands at (1047 and 1064 cm^{-1}), (1321 and 1388 cm^{-1}), (1643 and 1616 cm^{-1}), and (3425 and 3438 cm^{-1}). In this study, the intense band pattern at 1047 and 1064 cm^{-1} was characteristic of C – OH stretching of secondary alcohols. The peaks 1321 and 1388 cm^{-1} correspond to C – N stretching vibrations of aromatic amines. The absorption peaks located at 1643 and 1616 cm^{-1} were identified as the amide I and arose due to the carbonyl stretch vibrations in the amide linkages of the proteins. The broad peaks of 3425 and 3438 cm^{-1} corresponding to NH stretching in amide (II) were observed in gold NPs and in the aqueous seed extract of *A. esculentus*, respectively. In this study, the FTIR spectrum results have shown that the extracts containing OH as a functional group act in capping the NPs synthesis.

3.3 Factors Affecting the Fabrication

During the fabrication of gold NPs, the challenges frequently encountered are (a) to control the particles' shape and size and (b) to achieve monodispersity in solution phase. The size, shape, and stability of gold NPs are influenced by various factors such as incubation time, temperature, pH, pressure, and concentration of plant extract/biomass and the gold solution**.** The desired morphology of NPs can be achieved by altering these growth factors in the synthesis medium. The major works related to the control of growth factors have been summarized in Table 3.2, and a brief account of these studies is given below.

Table 3.2 Effect of the relevant factors (temperature, pH, and incubation time of the solution) on the particle shape during the plant-mediated fabrication of gold nanoparticles

Level	Shapes	References
25 °C	Triangular	Song et al. (2009)
60 °C	Pentagonal	Song et al. (2009)
90 °C	Hexagonal	Song et al. (2009)
30 °C	Spherical, triangle, truncated triangles, and decahedral	Narayanan and Sakthivel (2010b)
Room temperature	Polydisperse with spherical, triangular, and hexagonal	Noruzi et al. (2011)
80 °C	Spherical	Das et al. (2011)
50 °C	Spherical, nanoprisms, nanotriangles, hexagons, trapezoids	Ghosh et al. (2012)
40 °C	Spherical	Gonnelli et al. (2015)
100 °C	Spherical	Mishra et al. (2016)
pH 4.8	Spherical	Sharma et al. (2007)
pH 9	Spherical	Castro et al. (2011)
pH 10	Rod shaped	Castro et al. (2011)
pH 11	Nanowires	Castro et al. (2011)
pH 2	Rod shaped, large	Armendariz et al. (2004)

Table 3.2 (continued)

Level	Shapes	References
pH 3–4	Rod shaped, small	Armendariz et al. (2004)
pH 8	Spherical, oval, polyhedral	Pasca et al. (2014)
pH 4–6	Spherical	Mishra et al. (2016)
5 h	Spherical	Chandran et al. (2006)
25 h	Triangular	Chandran et al. (2006)
0–6 days	Spherical	Sharma et al. (2007)
12 h	Spherical, triangular, truncated, decahedral	Narayanan and Sakthivel (2008)
2 min	Smaller, spherical	Philip (2010)
<5 min	Spherical, triangular, and hexagonal	Noruzi et al. (2011)
1 h	Spherical, triangle, truncated triangular, and decahedral	Narayanan and Sakthivel (2010b)
30 min	Spherical	Das et al. (2011)
20 min	Spherical	Kumar et al. (2011)
20 min	Spherical, nanoprisms, nanotriangles, hexagons, trapezoids	Ghosh et al. (2012)
20 s	Spherical	Kumar et al. (2012)
3 min	Spherical	Yasmin et al. (2014)
30 min	Spherical	Gonnelli et al. (2015)
6 min	Spherical	Mishra et al. (2016)

3.3.1 Temperature

Control of temperature is an important factor with respect to the shape and size of NPs in plant-mediated synthesis. During the gold NP fabrication from *Nyctanthes arbor-tristis* ethanolic flower extract, predominantly spherical NPs were obtained at high temperatures, while they assumed different shapes (triangular, pentagonal, rod-like, as well as spherical) at low temperatures (Das et al. 2011). This shape variation was ascribed to exposure of the nucleation procedure of metallic NPs to the reaction temperature. The high reaction rate at a high temperature more effectively facilitates the ingesting of gold ions in the establishment of nuclei, which could inhibit the secondary reduction process on the surface of the preformed nuclei, thus resulting in spherical particles. The secondary nucleation is favored at low temperature, which could result in particles of different shapes (Das et al. 2011). Similarly, Song et al. (2009) demonstrated a decrease in size of gold NPs synthesized by *Magnolia kobus* and *Diospyros kaki* leaf broth, when temperature was increased. They suggested that most of the gold ions were consumed in the formation of nuclei, and the secondary reduction phenomenon on the surface of nuclei was inhibited on increasing the temperature (Song et al. 2009). Thus, the suppression of secondary nucleation phenomenon at high temperatures might be a reason for the formation of particles with more uniform morphology. Gericke and Pinches (2006) obtained nanorod or platelet-shaped gold NPs at higher temperatures, while

spherical NPs at lower temperatures. Dubey et al. (2010b) noted that an increase in temperature from 25 to 150 °C leads to increase in the sharpness of absorption peaks for both gold and silver NPs in *Tanacetum vulgare* fruit extract. High temperature also increases the rate of reaction, which enhances NP fabrication (Phillip 2009; Dwivedi and Gopal 2010). As the sharpness in absorbance peak depends on the size of NPs, the small particle size at high temperature results in the sharpening of the plasmon resonance band of gold and silver NPs (Fayaz et al. 2009; Shaligram et al. 2009). Ghodake et al. (2010) used pear fruit extract for fabrication of gold nanoplates at room temperature. Ability to produce the metallic NPs at room temperature makes the processing easy and has the advantage of energy-saving. However, further investigation is still required regarding the control of shape and size of gold NPs by adjusting the temperature; availability of temperature-sensitive metabolites in the plant is of great importance in this context.

3.3.2 pH

Several studies have laid emphasis on the role of pH of reaction mixtures on the shape and size of particles during the NP fabrication from plant extracts. The reaction pH has the ability to change the electrical charges of biomolecules, which possibly affect their stabilizing and capping capabilities and then the NPs growth. This may help in forming the NPs of some particular shapes at a certain pH range so that a greater stability could be accomplished. However, extracts of various plants or different parts of the same plant species may have varying values of pH; hence optimization of fabrication process is desirable for an effective NP synthesis. Gardea-Torresdey et al. (1999) confirmed the significant role of pH in the fabrication of colloidal gold from alfalfa biomass and suggested that the NP size varies with the change in pH. This was endorsed by Mock et al. (2002). Armendariz et al. (2004) then examined the gold NPs biosynthesized with *Avena sativa* biomass and found their size to be highly dependent on the pH value. These authors obtained smaller gold NPs at pH values of 3 and 4 and the larger ones at pH 2. The process of gold NP aggregation to form the larger ones at pH 2 was ideal over the nucleation to form new NPs. However, at pH 3 and 4, perhaps more functional groups are accessible for Au(III) complexes to bind with the biomass at the same time, which facilitates the successive formation of larger amounts of NPs of smaller diameters. Nevertheless, at pH 5 the biomass carries an overall negative charge due to the functional group (carboxyl) available in the biomass. Thus, the negatively charged $[AuCl4]^-$ does not approach the binding sites easily, and this prevents the binding of Au(III) and its reduction to Au(0), leading to the formation of fewer NPs. Moreover, electrostatic repulsion may also prevent aggregation and growth of small NPs and, therefore, result in the formation of small gold NPs of irregular shape (Armendariz et al. 2004). Ghodake et al. (2010) used pear fruit extract for fabricating gold nanoplates and found that alkaline condition was more effective for triangular and hexagonal nanoplates, while the structures of these nanoplates were barely detected at acidic pH.

3.3.3 Incubation Time

Incubation time, i.e., the time duration needed for a successful achievement of all reaction steps, influences the fabrication process of NPs. For instance, in the case of *Tanacetum vulgare* fruit extract-mediated fabrication of silver and gold NPs, the reaction started within 10 min, and an increase in the incubation time led to the sharpening of peaks for these NPs (Dubey et al. 2010a, b). Dwivedi and Gopal (2010) also found that by increasing the gold salt concentration, the size of gold NPs could be increased. In addition, increase in the reaction temperature increased the reaction rate also. Using the extract of *Rosa* hybrid petals, Noruzi et al. (2011) recorded a higher rate of reaction in comparison to previous studies, as the gold NP fabrication process was finished within 5 min (Noruzi et al. 2011). However, using the *Terminalia chebula* plant extracts, Kumar et al. (2012) produced gold NPs in 20 s only.

3.3.4 Plant Biomass Concentration

The plant biomass and/or extract concentrations used during the formation of NPs is another significant factor, which regulates the level of reduction and stabilization by the biomolecules and affects the NP morphology, as noticed in the case of gold NPs obtained with the help of *Cymbopogon flexuosus* (Shankar et al. 2005). Anisotropic gold NPs were biosynthesized by the reaction of *C. flexuosus* extract with Au(III) ions. The size of nanotriangles could be changed by altering the extract concentration. As the extract amounts were increased, the size of the triangular and hexagonal particles decreased, whereas the ratio of the number of spherical NPs to triangular/hexagonal particles increased. Song et al. (2009) used *Magnolia kobus* and *Diospyros kaki* leaf extracts for the biosynthesis of gold NPs. At higher extract concentrations, smaller and mainly spherical NPs were formed, while a variety of other morphologies in larger sizes were produced at lower extract concentrations. Kasthuri et al. (2009) also reported a change in particle morphology with the phyllanthin-assisted and clove extract-assisted biosynthesis of gold NPs. At lower concentrations of plant extract, particle size increased, and hexagonal or triangular gold NPs were formed. Dubey et al. (2010a) used the aqueous extract of *Sorbus aucuparia* leaf for the synthesis of silver and gold NPs. They recorded an accelerated particle formation and a reduced size of both the silver and gold nanocolloids when the amount of extract was increased. Similarly, an increase in the amount of the *Chenopodium album* leaf extract caused a decrease in the particle size (Dwivedi and Gopal 2010). During the biosynthesis of gold NPs with the help of *Sapindus mukorossi* extract, few aggregations and heterogeneous structures were observed at a lower (15%) concentration, while spherical NPs and more dispersion occurred at a higher (45%) concentration (Reddy et al. 2012).

3.4 Applications of Gold Nanoparticles

The use of gold NPs for staining of glass and enamels and for treating certain diseases dates back to the sixteenth century. Now their applications are common in biomedicine, bio-sensing, catalysis, agriculture, electronic and magnetic devices, etc. (Husen and Siddiqi 2014; Husen 2017; Siddiqi and Husen 2017a; Ovais et al. 2017). As they are nontoxic and readily adsorb on DNA, Au NPs are used for bombardment during delivery of genetic materials into plants (Moaveni et al. 2011) and in the quantitative determination of heavy metals (Liu and Lu 2003), blood glucose (Luo et al. 2004), and pesticides (Lisha and Pradeep 2009). Their applications in various areas are discussed below and shown in Fig. 3.11.

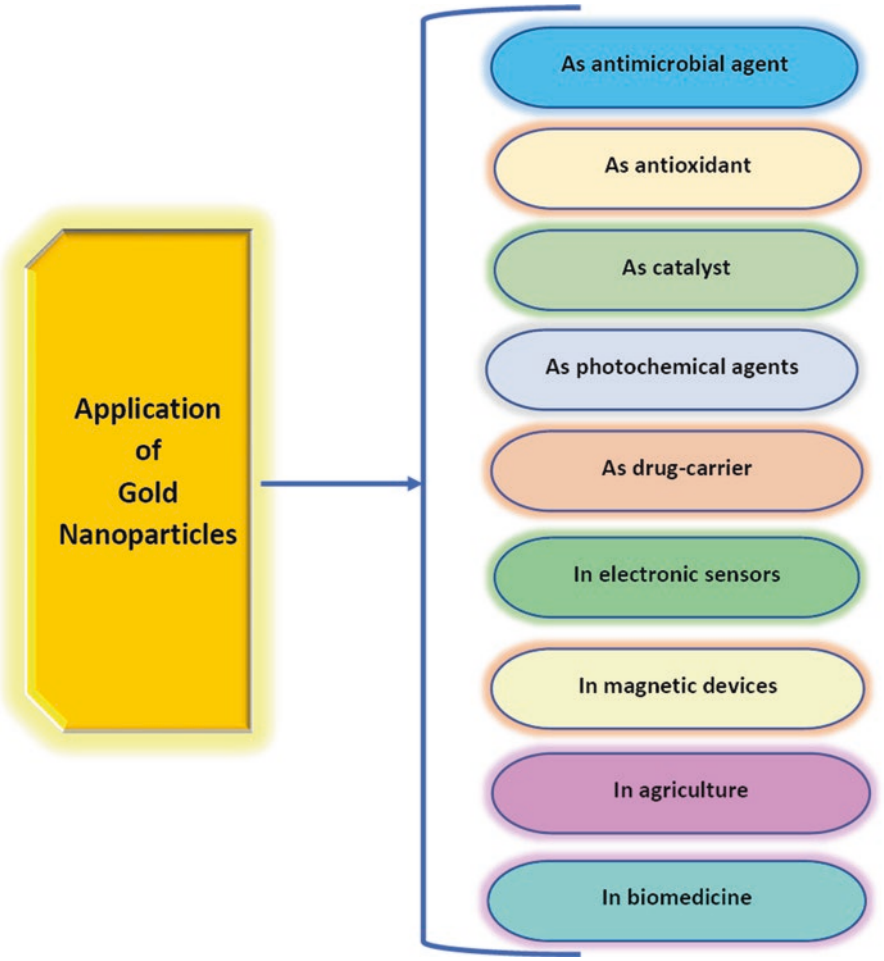

Fig. 3.11 Various applications of gold nanoparticles

3.4.1 Antimicrobial Agents

Microbial resistance to antibiotics has an undesirable consequence on human health by causing side effects due to consumption of higher drug doses and/or a prolonged treatment period. The biosynthesized NPs offer an auspicious solution in the drug-resistance management. Gold NPs fabricated with plant material have shown strong antimicrobial activity (Sreelakshmi et al. 2011; Husen and Siddiqi 2014; Piruthiviraj et al. 2016; Balasubramani et al. 2017). The growth of gram-negative and gram-positive bacteria was effectively inhibited with functionalized gold NPs (Li et al. 2014). The gold and silver NPs produced from *Mentha piperita* have shown a strong antibacterial effect against *Staphylococcus aureus* and *Escherichia coli* (Ali et al. 2011). Similar impact of honey-mediated gold and silver NPs was noticed by Sreelakshmi et al. (2011). Gold NPs obtained from *Brassica oleracea* also suppressed the growth of bacteria (*Staphylococcus aureus*, *Klebsiella pneumonia*) and fungi (*Aspergillus flavus*, *A. niger*, and *Candida albicans*) (Piruthiviraj et al. 2016). Their antimicrobial efficiency was comparable with that of the standard drugs gentamicin and fluconazole. In a recent study, bioactivity of *Nitzschia (*diatom)-fabricated gold NPs was examined by coupling them with antibiotics such as penicillin and streptomycin; the antibacterial potential of the combination against *Escherichia coli*, *Pseudomonas aeruginosa*, and *Staphylococcus aureus* was greater than that of either NPs or antibiotics alone (Borase et al. 2017). In another study, the gold and silver NPs produced with the *Mussaenda glabrata* aqueous leaf extract were found effective in inhibiting the pathogenic microbes *such as Bacillus pumilus*, *Staphylococcus aureus*, *Pseudomonas aeruginosa*, *Escherichia coli*, *Aspergillus niger*, and *Penicillium chrysogenum* (Francis et al. 2017a, b).

3.4.2 Catalytic Activity and Water Purification

Enormous use of toxic organic chemicals leads to water pollution. Over 7×10^5 tons of about 10,000 different types of dyes and pigments, most of which are carcinogenic, is produced worldwide every year. It is estimated that 10–15% of the dye is lost in the effluent during the dyeing process (Gupta et al. 2011). The silver and gold nanocatalysts are efficient to clean these cancer-causing dyes from water bodies using the electron-relay effects (Joseph and Mathew 2015b; Lim et al. 2016). Ramakrishna et al. (2016) have produced gold NPs using marine algae as catalyst in the reduction of various nitro compounds. Francis et al. (2017a, b) have fabricated gold and silver NPs from *Mussaenda glabrata* aqueous leaf extract and used them as heterogeneous catalysts in different dye degradation processes. Several other reports highlight the use of gold NPs as catalyst for selective reactions at low temperature, viz., the water gas shift reaction and selective oxidation of carbon monoxide (Andreeva 2002; Grisel et al. 2002; Hutchings and Haruta 2005), glycerol (Carrettin et al. 2002), and methanol (Hernández et al. 2006), hydrogenation of

unsaturated materials (Claus et al. 2000), and reduction of aromatic nitro compounds (Kundu et al. 2009) and a toxic pollutant 4-nitrophenol to 4-aminophenol (Ghosh et al. 2012; Yu et al. 2016). Gold NPs of different sizes fabricated with the *Tribulus terrestris* fruit extract exhibited catalytic reduction of p-nitroaniline to p-phenylenediamine (Gopinath et al. 2019). Recently, Manjari et al. (2017) achieved an ultrarapid homogeneous and heterogeneous complete degradation of methylene blue and Congo red within few seconds by using as catalyst the silver and gold NPs fabricated with the *Aglaia elaeagnoidea* flower extract. They found above 90% conversion of 4-nitrophenol to 4-aminophenol within few minutes for homogenous and within few seconds for heterogeneous degradation. Pradeep and Anshup (2009) also found gold NPs suitable for the removal of heavy metals through alloy formation by varying the composition such as Au_3Hg, AuHg, and $AuHg_3$ phases; thus these NPs can be used for removing Hg ions from contaminated water. Gold NPs are also used for the detection and removal of organic compounds such as pesticides like malathion, endosulfan, and chlorpyrifos (Han et al. 2003; Nair et al. 2003). Burns et al. (2006) noted that salt-induced aggregation of gold NPs is useful for detecting pesticides at low concentration and removing them from drinking water. Furthermore, removal of diesel oil droplets floating on water through swelling and absorption of the gold NP composite has also been observed (Gupta and Kulkarni 2011). All these findings have a lot of promise for the wastewater purification by degrading its toxic contaminants.

3.4.3 Antioxidant Potential

Oxidation is a process in which free radicals are generated due to chemical reaction; free radicals cause damage to cells and disturb their functioning. Antioxidants are known to prevent cell damage, DNA damage, malignant transformation, heart diseases, cancer, and oxidative stress (Watters et al. 2007). Both natural and synthetic antioxidants are used to cure these problems. Anagnostopoulou et al. (2006) and Carocho and Ferreira (2013) have suggested that the synthetic antioxidants are suspected to cause adverse health effects. In a study, Au NP-embedded flavones with other dietary nutrients have exhibited significant enhancement in the antioxidant activity (Medhe et al. 2014). Leu et al. (2012) have reported that the antioxidative ability of known antioxidants was much increased when used in combination with gold NPs for the purpose of wound healing. Abel et al. (2016) produced gold NPs from the *Cassia tora* secondary metabolite conjugate and noted their higher bioavailability and the antioxidant and anticancer effect against the colon cancer cell line (Col320). Manjari et al. (2017) found enhanced antioxidant activity on increasing the concentration of gold and silver NPs obtained from the *Aglaia elaeagnoidea* flower extract. Sathish et al. (2016) have reported extraordinary antioxidant potential of gold NPs produced by using the aqueous fruit extract of *Couroupita guianensis*. Balasubramani et al. (2015) found the *Antigonon leptopus*-mediated gold NPs as a free radical scavenger and an anticancer agent.

3.4.4 Photochemical Agents

Gold NPs are used as inert carriers to modify the excited state photochemistry and prevent the unwanted phototoxicity effects of the adsorbed drug molecules (Wang et al. 2016). A study of the uptake of gold NPs by *Arabidopsis thaliana* roots and their subsequent translocation to leaves has shown the generation of nanobubbles and acoustic signals in plant tissues (Koo et al. 2016). In addition, the leaves containing gold NPs exhibited a higher temperature across the leaf surface and induced expression of heat shock-regulated genes, when exposed to laser beam. These results demonstrate that gold NPs in the leaves can act as the photochemical agents and raise the leaf temperature by absorbing the light waves to induce photochemical activity even when the temperature is very low.

3.4.5 Plant Response to Gold Nanoparticles

Being stationary and having a large leaf area, plants are prone to exposure to a wide range of NPs available in their surrounding environment (Dietz and Herth 2011). They significantly control metal ions or NPs by accumulating them into their biomass (Husen and Siddiqi 2014; Iqbal et al. 2015; Siddiqi and Husen 2016). Upon entering into plants, gold NPs may activate or prevent plant growth and biomass accumulation. In general, higher doses of gold solutions may cause toxicity and thus affect the plant growth negatively, producing changes at the physiological, biochemical, and molecular levels (Siddiqi and Husen 2016). Although treatment of *Arabidopsis thaliana* root with a lower dose (10 ppm $KAuCl_4$) markedly increased the root length, a significant decrease was noted at higher doses (25, 50 and100 ppm). Further, at higher concentrations of $KAuCl_4$, iron content was depleted, while Zn and P contents declined (Jain et al. 2014). Another study of *A. thaliana* revealed a significant role of gold NPs in seed germination, modulation of antioxidant system, and regulation of microRNA expression that controls different morphological, physiological, and metabolic processes (Kumar et al. 2013). Judy et al. (2012) recorded accumulation of 2–54 μg gold g^{-1} in the dried tobacco plants after their exposure for 7 days to 30 μg gold mL^{-1} in the nutrient solution.

Earlier, Barrena et al. (2009) found a low or zero toxicity of the gold, silver, and magnetite NPs at concentrations of 62, 100, and 116 μg mL^{-1}, respectively, in cucumber and lettuce plants. Many other studies have also shown that gold can accumulate to varying degrees in different plant species such as *Brassica juncea*, *B. campestris*, *Trifolium repens*, *Sorghum helense*, *Raphanus sativus*, *Kalanchoe serrata*, and *Helianthus annuus* (Wilson-Corral et al. 2012; Siddiqi and Husen 2016). Gold NP application improved the seed germination in cucumber and lettuce (Barrena et al. 2009), *Brassica juncea* (Arora et al. 2012) and *Gloriosa superba* (Gopinath et al. 2014). *B. juncea* seedlings exhibited changes both in growth and seed yield; foliar spray of gold NPs enhanced the oil production with a concomitant

decline in reducing sugar and total sugar contents (Arora et al. 2012). Redox status of the treated *B. juncea* was also improved. Seed germination percentage increased with spray and/or inoculation with 25 ppm gold NPs, but the higher concentrations had a negative impact. Gunjan et al. (2014) reported that gold NPs (in 100–400 ppm doses) reduced the *B. juncea* growth possibly due to rise in free radical stress, as indicated by the general rise in activities of antioxidative enzymes, viz., catalase, ascorbate peroxidase, guaiacol peroxidase, and glutathione reductase. Furthermore, proline and hydrogen peroxide contents were also enhanced due to the formation of reactive oxygen species (ROS). These observations suggest that the ROS production, which makes for the physiological and biochemical stress in plants, is dependent on the dose of gold NPs. Of late, Balalakshmi et al. (2017) produced spherical, 25 nm gold NPs, using *Sphaeranthus indicus*, and examined them at 0, 1, 3, 5, 7, and 10% concentrations of the plant *extract* for the mitotic cell division assays, pollen germination experiments, and in vivo toxicity trials against an aquatic crustacean. In this experiment, gold NPs did not show any toxic effects on plant cells and aquatic crustacean. Most of the studies on plant responses to gold NPs have so far been focused on early stages of plant growth (Siddiqi and Husen 2016). Random application of metal particles may not produce the desired results with reference to plant growth or yield. It is necessary to identify which trace elements are useful for a given plant species so that the same may be used in the form of NPs to increase the quality and quantity of plant products.

3.4.6 Biomedical Application

Gold NPs are successfully used for transporting drugs, genes, and other biomolecules due to their low toxicity, high surface area, and tunable stability. For instance, gold NPs with 2 nm core diameter have been used as carrier in the preparation of the chemotherapeutic drug agent, paclitaxel (Gibson et al. 2007). Moreover, their tunable size and functionality also allow them to work as a useful scaffold for the delivery of peptides, proteins, or nucleic acids like DNA or RNA (Bhumkar et al. 2007; Ghosh et al. 2008; Rana et al. 2012; Ding et al. 2014). They were also adhered to the vascular endothelial growth factor antibodies, which are used in treating the B-chronic lymphocytic leukemia (Mukherjee et al. 2007). Gold NPs are conjugated oligonucleotide/DNA and employed in clinical diagnosis and colorimetric detection of targeted DNA, virus, etc. (Upadhyay et al. 2006; Baptista et al. 2008; Costa et al. 2010; Nun et al. 2013). Gold NP-bifunctional oligonucleotide probe conjugate for the detection of dsDNA even in very minute quantity has also been reported (Dharanivasan et al. 2016). Thanh and Rosenzweig (2002) developed a unique, sensitive, and highly specific immunoassay system for antibodies by using gold NPs. The colloidal gold NPs transmit drug to the site of the use regardless of their shape, if both of them (NPs and drug) are biocompatible, stable, and easily form bonds with each other. They are finally deposited in cells and on irradiation with visible light; the heat mediated by gold NPs destroys the cancerous tissues locally (Huang

et al. 2006; Huff et al. 2007; Lowery et al. 2006). They are also used in the Carter-Wallace home pregnancy's "First Response" kit. During its use, when the latex micro- and gold NPs derivatized with a hormone released by pregnant women were mixed, the micro- and nanoparticles coagulated, forming clumps of pink color (Bangs 1996). Bio-detection sensitivity obtained from spherical NPs was not strong enough to trace the interaction of biomolecules (Orendorff et al. 2005). In its place, irregular-shaped NPs could improve the biological detection sensitivity greatly. NP fabrication from plants may give irregular-shaped nanostructures in a one-pot process due to the complexity of the bio-reducing and bio-capping agents (Lukman et al. 2011).

Thus, NPs fabricated with the help of plants have a potential and could be utilized in various applications that need irregular shape of nanostructures. Raman spectroscopy is a vibrational method for collecting information about the chemical structure (González-Solís et al. 2013). Gold NPs also increase the intensity of Raman scattering of adjacent molecules and hence are extensively used in surface-enhanced Raman scattering (SERS) for the detection and quantitative analysis of Raman active materials (Qian and Nie 2008; Zamarion et al. 2008; Dasary et al. 2009; Ding et al. 2013). This technique is used to increase the sensitivity and reproducibility of the analyses (Kumar and Yadav 2009). SERS technique is used to distinguish cancer cells from normal cells, when gold nanorods conjugate to anti-epidermal growth factor receptor antibodies (Huang et al. 2007b). SERS with gold NPs has been employed in cancer research to detect tumors (Cai et al. 2008; Huang and El-Sayed 2010) and in immunoassays as well as the examination of living cells (Kneipp et al. 2002; Grubisha et al. 2003; Neng et al. 2010). Gold NPs have also been used in the cell and phantom imaging (Huang et al. 2007b; Cai et al. 2008), mostly during cell culture studies. Peleg et al. (1999) have reported the benefit of the enhanced second harmonic signal by antibody-conjugated gold NPs for functional cellular imaging around single molecules. Krishnaraj et al. (2014) have reported the in vitro cytotoxic effect of silver and gold NPs (obtained by an *Acalypha indica-mediated* synthesis) against the MDA-MB-231, human breast cancer cells, and could cause significant cytotoxic effects and apoptotic features. Subsequently, many other research groups have reported anticancer properties of plant-mediated gold NPs such as those involving *Moringa oleifera* (Anand et al. 2015; Tiloke et al. 2016), *Portulaca grandiflora (*Ashokkumar et al. 2016), *Musa paradisiaca* (Vijayakumar et al. 2017), *Spinacia oleracea* (Ramachandran et al. 2017), and so on.

3.5 Conclusion

The principal biomolecules in plant extracts, which are responsible for the reduction of metal ions to form NPs, include amines, amino acids, aldehydes, ketones, carboxylic acids, phenols, proteins, flavonoids, saponins, steroids, alkaloids, tannins, vitamins, etc. The complex nature of plant extracts and their involvement in the gold

NP fabrication require a comprehensive investigation. Many factors such as incubation time, temperature, plant extract concentration, pH values, etc. affect the growth, morphology, and stability of particles. Optimization techniques for a homogenous production of gold NPs are needed for better processing and application in various sectors. The random and excessive use of gold NPs may not give the desired output in terms of plant growth and yield in all the species and may rather lead to ecological risks. It is essential to explore which specific metal/trace element works well with which species, so that NPs of the same material may be used to increase the quality and quantity of plant products in a cost-effective manner.

References

Abel EE, Poonga PRJ, Panicker SG (2016) Characterization and in vitro studies on anticancer, antioxidant activity against colon cancer cell line of gold nanoparticles capped with *Cassia tora* SM leaf extract. Appl Nanosci 6:121–129

Ali MD, Thajuddin N, Jeganathan K, Gunasekaran M (2011) Plant extract mediated synthesis of silver and gold nanoparticles and its antibacterial activity against clinically isolated pathogens. Colloids Surf B Biointerfaces 85:360–365

Anagnostopoulou MA, Kefalas P, Papageorgiou VP, Assimopoulou AN, Boskou D (2006) Radical scavenging activity of various extracts and fractions of sweet orange peel (Citrus sinensis). J Food Chem 94:19–25

Anand K, Gengan RM, Phulukdaree A, Chuturgoon A (2015) Agroforestry waste *Moringa oleifera* petals mediated green synthesis of gold nanoparticles and their anti-cancer and catalytic activity. J Ind Eng Chem 21:1105–1111

Andreeva D (2002) Low temperature water gas shift over gold catalysts. Gold Bull 35:82–88

Ankamwar B (2010) Biosynthesis of gold nanoparticles (green-gold) using leaf extract of *Terminalia Catappa*. E-J Chem 7:1334–1339

Annamalai A, Christina VLP, Sudha D, Kalpana M, Lakshmi PTV (2013) Green synthesis, characterization and antimicrobial activity of Au NPs using *Euphorbia hirta* L. leaf extract. Colloids Surf B: Biointerfaces 108:60–65

Armendariz V, Herrera I, Peralta-Videa JR, Jose-Yacaman M, Troiani H, Santiago P, Gardea-Torresdey JL (2004) Size controlled gold nanoparticle formation by Avena sativa biomass: use of plants in nanobiotechnology. J Nano Res 6:377–382

Arora S, Sharma P, Kumar S, Nayan R, Khanna PK, Zaidi MGH (2012) Gold-nanoparticle induced enhancement in growth and seed yield of *Brassica juncea*. Plant Growth Regul 66:303–310

Ashokkumar T, Arockiaraj J, Vijayaraghavan K (2016) Biosynthesis of gold nanoparticles using green roof species *Portulaca grandiflora* and their cytotoxic effects against C6 glioma human cancer cells. Environ Prog Sustain Energy 35:1732–1740

Babu PJ, Saranya S, Sharma P, Tamuli R, Bora U (2012) Gold nanoparticles: sonocatalytic synthesis using ethanolic extract of *Andrographis paniculata* and functionalization with polycaprolactone–gelatin composites. Front Mater Sci 6:236–249

Balalakshmi C, Gopinath K, Govindarajan M, Lokesh R, Arumugam A, Alharbi NS, Kadaikunnan S, Khaled JM, Benelli G (2017) Green synthesis of gold nanoparticles using a cheap *Sphaeranthus indicus* extract: impact on plant cells and the aquatic crustacean *Artemia nauplii*. J Photochem Photobiol B 173:598–605

Balasubramani G, Ramkumara R, Krishnaveni N, Pazhanimuthu A, Natarajan T, Sowmiya R, Perumal P (2015) Structural characterization, antioxidant and anticancer properties of gold nanoparticles synthesized from leaf extract (decoction) of *Antigonon leptopus* Hook. & Arn. J Trace Elem Med Biol 30:83–89

Balasubramani G, Ramkumar R, Raja RK, Aiswarya D, Rajthilak C, Perumal P (2017) *Albizia amara* Roxb. Mediated gold nanoparticles and evaluation of their antioxidant, antibacterial and cytotoxic properties. J Clust Sci 28:259–275

Bali R, Harris AT (2010) Biogenic synthesis of Au nanoparticles using vascular plants. Ind Eng Chem Res 49:12762–12772

Bangs LB (1996) New developments in particle-based immunoassays: introduction. Pure Appl Chem 68:1873–1879

Baptista P, Pereira E, Eaton P, Doria G, Miranda A, Gomes I, Quaresma P, Franco R (2008) Gold nanoparticles for the development of clinical diagnosis methods. Anal Bioanal Chem 391:943–950

Barrena R, Casals E, Colón J, Font X, Sánchez A, Puntes V (2009) Evaluation of the ecotoxicity of model nanoparticles. Chemosphere 75:850–857

Begum NA, Mondal S, Basu S, Laskar RA, Mandal D (2009) Biogenic synthesis of Au and Ag nanoparticles using aqueous solutions of *Black Tea* leaf extracts. Colloids Surf B Biointerfaces 71:113–118

Bhumkar DR, Joshi HM, Sastry M, Pokharkar VB (2007) Chitosan reduced gold nanoparticles as novel carriers for transmucosal delivery of insulin. Pharm Res 24:1415–1426

Bindhani BK, Panigrahi AK (2014) Green synthesis and characterization of gold nanoparticles using leaf extracts of *Withania somnifera* (Linn.) (Ashwagandha). Int J Mat Sci Appl 3:279–284

Borase HP, Patil CD, Suryawanshi RK, Koli SH, Mohite BV, Benelli G, Patil SV (2017) Mechanistic approach for fabrication of gold nanoparticles by *Nitzschia* diatom and their antibacterial activity. Bioprocess Biosyst Eng 40:1437–1446

Boxi SS, Mukherjee K, Paria S (2016) Ag doped hollow TiO_2 nanoparticles as an effective green fungicide against *Fusarium solani* and *Venturia inaequalis* phytopathogens. Nanotechnology 27:085103–085116

Burns C, Spendel WU, Puckett S, Pacey GE (2006) Solution ionic strength effect on gold nanoparticle solution color transition. Talanta 69:873–876

Cai W, Gao T, Hong H, Sun J (2008) Applications of gold nanoparticles in cancer nanotechnology. Nanotechnol Sci Appl 1:17–32

Carocho M, Ferreira ICFR (2013) A review on antioxidants, prooxidants and related controversy: natural and synthetic compounds, screening and analysis methodologies and future perspectives. Food Chem Toxicol 51:15–25

Carrettin S, McMorn P, Johnston P, Griffin K, Hutchings GJ (2002) Selective oxidation of glycerol to glyceric acid using a gold catalyst in aqueous sodium hydroxide. Chem Commun 7:696–697

Castro L, Blazquez ML, Munoz JA, Gonzalez F, Garcia-Balboa C, Ballester A (2011) Biosynthesis of gold nanowires using *sugar beet* pulp. Process Biochem 46:1076–1082

Chandran SP, Chaudhary M, Pasricha R, Ahmad A, Sastry M (2006) Synthesis of gold nanotriangles and silver nanoparticles using *Aloe vera* plant extract. Biotechnol Prog 22:577–583

Chandran K, Song S, Yun SII (2014) Effect of size and shape controlled biogenic synthesis of gold nanoparticles and their mode of interactions against food borne bacterial pathogens. Arab J Chem. https://doi.org/10.1016/j.arabjc.2014.11.041

Claus P, Brückner A, Mohr C, Hofmeister H (2000) Supported gold nanoparticles from quantum dot to mesoscopic size scale: effect of electronic and structural properties on catalytic hydrogenation of conjugated functional groups. J Am Chem Soc 122:11430–11439

Costa P, Amaro A, Botelho V, Inacio J, Baptista PV (2010) Gold nanoprobe assay for the identification of mycobacteria of the Mycobacterium tuberculosis complex. Clin Microbiol Infect 16:1464–1469

Daizy P (2009) Honey mediated green synthesis of gold nanoparticles. Spectrochim Acta A Mol Biomol Spectrosc 73:650–653

Das RK, Gogoi N, Bora U (2011) Green synthesis of gold nanoparticles using *Nyctanthes arbortristis* flower extract. Bioprocess Biosyst Eng 34:615–619

Dasary SS, Singh AK, Senapati D, Yu H, Ray PC (2009) Gold nanoparticle based label-free SERS probe for ultrasensitive and selective detection of trinitrotoluene. J Am Chem Soc 131:13806–13812

Dash SS, Bag BG (2014) Synthesis of gold nanoparticles using renewable *Punica granatum* juice and study of its catalytic activity. Appl Nanosci 4:55–59

Dharanivasan G, Riyaz SUM, Jesse DMJ, Muthuramalingam TR, Rajendran G, Kathiravan K (2016) DNA templated self-assembly of gold nanoparticle clusters in the colorimetric detection of plant viral DNA using a gold nanoparticle conjugated bifunctional oligonucleotide probe. RSC Adv 6:11773–11785

Dietz KJ, Herth S (2011) Plant nanotoxicology. Trends Plant Sci 16:582–589

Ding X, Kong L, Wang J, Fang F, Li D, Liu J (2013) Highly sensitive SERS detection of Hg2+ ions in aqueous media using gold nanoparticles/graphene heterojunctions. ACS Appl Mater Interfaces 5:7072–7078

Ding Y, Jiang Z, Saha K, Kim CS, Kim ST, Landis RF, Rotello VM (2014) Gold nanoparticles for nucleic acid delivery. Mol Ther 22:1075–1083

Dubey SP, Lahtinen M, Särkkä H, Sillanpää M (2010a) Bioprospective of *Sorbus aucuparia* leaf extract in development of silver and gold nanocolloids. Colloids Surf B Biointerfaces 80:26–33

Dubey SP, Lahtinen M, Sillanpaa M (2010b) Tansy fruit mediated greener synthesis of silver and gold nanoparticles. Process Biochem 45:1065–1071

Dwivedi AD, Gopal K (2010) Biosynthesis of silver and gold nanoparticles using *Chenopodium album* leaf extract. Colloids Surf A Physicochem Eng Asp 369:27–33

Fayaz AM, Balaji K, Kalaichelvan PT, Venkatesan R (2009) Fungal based synthesis of silver nanoparticles-an effect of temperature on the size of particles. Colloids Surf B Biointerfaces 74:123–126

Fayaz AM, Girilal M, Venkatesan R, Kalaichelvan PT (2011) Biosynthesis of anisotropic gold nanoparticles using Maduca longifolia extract and their potential in infrared absorption. Colloids Surf B Biointerfaces 88:287–291

Fraceto LF, Grillo R, de Medeiros DGA, Scognamiglio V, Rea G, Bartolucci C (2016) Nanotechnology in agriculture: which innovation potential does it have? Front Environ Sci 4:20–25

Francis S, Joseph S, Koshy EP, Mathew B (2017a) Green synthesis and characterization of gold and silver nanoparticles using *Mussaenda glabrata* leaf extract and their environmental applications to dye degradation. Environ Sci Pollut Res 24:17347–17357

Francis S, Joseph S, Koshy EP, Mathew B (2017b) Synthesis and characterization of multifunctional gold and silver nanoparticles using leaf extract of *Naregamia alata* and their applications to catalysis and control of mastitis. New J Chem 41:14288–14298

Gardea-Torresdey JL, Tiemann KJ, Gamez G, Dokken K, Tehuacamanero S, Jose-Yacaman M (1999) Gold nanoparticles obtained by bio-precipitation from gold (III) solutions. J Nanopart Res 1:397–404

Gardea-Torresdey JL, Parsons JG, Gomez E, Peralta-Videa J, Troiani HE, Santiago P, Yacaman MJ (2002) Formation and growth of au nanoparticles inside live alfalfa plants. Nano Lett 2:397–401

Gardea-Torresdey JL, Gomez E, Peralta-Videa JR, Parsons JG, Troiani H, Jose-Yacaman M (2003) Alfalfa sprouts: a natural source for the synthesis of silver nanoparticles. Langmuir 19:1357–1361

Geetha R, Kumar TA, Tamilselvan S, Govindaraju K, Sadiq M, Singaravelu G (2013) Green synthesis of gold nanoparticles and their anticancer activityCancer. Nano 4:91–98

Gericke M, Pinches A (2006) Biological synthesis of metal nanoparticles. Hydrometallurgy 83:132–140

Ghodake GS, Deshpande NG, Lee YP, Jin ES (2010) Pear fruit extract-assisted room-temperature biosynthesis of gold nanoplates. Colloids Surf B Biointerfaces 75:584–589

Ghosh P, Han G, De M, Kim CK, Rotello VM (2008) Gold nanoparticles in delivery applications. Adv Drug Deliv Rev 60:1307–1315

Ghosh S, Patil S, Ahire M, Kitture R, Gurav DD, Jabgunde AM, Kale S, Pardesi K, Shinde V, Bellare J, Dhavale DD, Chopade BA (2012) *Gnidia glauca* flower extract mediated synthesis of gold nanoparticles and evaluation of its chemocatalytic potential. J Nanobiotechnol 10:17

Gibson JD, Khanal BP, Zubarev ER (2007) Paclitaxel-functionalized gold nanoparticles. J Am Chem Soc 129:11653–11661

Gonnelli C, Cacioppo F, Cristiana G, Capozzoli L, Salvatici C, Salvatici MC, Colzi I, Bubba MD, Ancillotti C, Ristori S (2015) *Cucurbita pepo* L. extracts as a versatile hydrotropic source for the synthesis of gold nanoparticles with different shapes. Green Chem Lett Rev 8:39–47

González-Ballesteros N, Prado-López S, Rodríguez-González JB, Lastra M, Rodríguez-Argüelles MC (2017) Green synthesis of gold nanoparticles using brown algae *Cystoseirabaccata*: its activity in colon cancer cells. Colloids Surf B Biointerfaces 153:190–198

González-Solís JL, Luévano-Colmenero GH, Vargas-Mancilla J (2013) Surface enhanced Raman spectroscopy in breast cancer cells. Laser Ther 22:37–42

Gopinath K, Venkatesha KS, Ilangovana R, Sankaranarayanan K, Arumugama A (2013) Green synthesis of gold nanoparticles from leaf extract of *Terminalia arjuna* for the enhanced mitotic cell division and pollen pollen germination activity. Ind Crop Prod 50:737–742

Gopinath K, Gowri S, Karthika V, Arumugam A (2014) Green synthesis of gold nanoparticles from fruit extract of *Terminalia arjuna* for the enhanced seed germination activity of Gloriosa superb. J Nanostruct Chem 4:115–125

Gopinath V, Priyadarshini S, Ali MD, Loke MF, Thajuddin N, Alharbi NS, Yadavalli T, Alagiri M, Vadivelu J (2019) Anti-helicobacter pylori, cytotoxicity and catalytic activity of biosynthesized gold nanoparticles: multifaceted application. Arab J Chem 12:33–40

Grisel R, Weststrate KJ, Gluhoi A, Nieuwenhuys BE (2002) Catalysis by gold nanoparticles. Gold Bull 35:39–45

Grubisha DS, Lipert RJ, Park H-Y, Driskell J, Porter MD (2003) Femtomolar detection of prostate-specific antigen: an immunoassay based on surface-enhanced Raman scattering and immuno-gold labels. Anal Chem 75:5936–5943

Gunjan B, Zaidi MGH, Sandeep A (2014) Impact of gold nanoparticles on physiological and biochemical characteristics of *Brassica juncea*. J Plant Biochem Physiol 2:133–138

Gupta R, Kulkarni GU (2011) Removal of organic compounds from water by using a gold nanoparticle-poly(dimethylsiloxane) nanocomposite foam. ChemSusChem 4:737–743

Gupta VK, Jain R, Saleh TA, Nayak A, Malathi S, Agarwal S (2011) Equilibirum and thermodynamic studies on the removal and recovery of Safranine-T Dye from industrial effluents. Sep Sci Technol 46:839–846

Han A, Dufva M, Belleville E, Christensen CB (2003) Detection of analyte binding to microarrays using gold nanoparticle labels and a desktop scanner. Lab Chip 3:329–332

Hernández J, Solla-Gullón J, Herrero E, Aldaz A, Feliu JM (2006) Methanol oxidation on gold nanoparticles in alkaline media: unusual electrocatalytic activity. Electrochim Acta 52:1662–1669. http://www.cytodiagnostics.com/store/pc/Introduction-to-Gold-Nanoparticle-Characterization-d3.htm (as Assessed on 3 December, 2017)

Huang X, El-Sayed MA (2010) Gold nanoparticles: optical properties and implementations in cancer diagnosis and photothermal therapy. J Adv Res 1:13–28

Huang XH, Jain PK, El-Sayed IH, El-Sayed MA (2006) Determination of the minimum temperature required for selective photothermal destruction of cancer cells with the use of immune targeted gold nanoparticles. Photochem Photobiol 82:412–417

Huang J, Li Q, Sun D, Lu Y, Su Y, Yang X, Wang H, Wang Y, Shao W, He N, Hong CC (2007a) Biosynthesis of silver and gold nanoparticles by novel sundried *Cinnamomum camphora* leaf. Nanotechnology 18:105104–105115

Huang X, El-Sayed IH, Qian W, El-Sayed MA (2007b) Cancer cells assemble and align gold nanorods conjugated to antibodies to produce highly enhanced, sharp, and polarized surface Raman spectra: a potential cancer diagnostic marker. Nano Lett 7:1591–1597

Huff TB, Tong L, Zhao Y, Hansen MN, Cheng JX, Wei A (2007) Hyper thermic effects of gold nanorods on tumor cells. Nanomedicine (Lond) 2:125–132

Husen A (2017) Gold nanoparticles from plant system: synthesis, characterization and their application. In: Ghorbanpour M, Manika K, Varma A (eds) Nanoscience and plant–soil systems, vol 48. Springer, Cham, pp 455–479

Husen A, Siddiqi KS (2014) Phytosynthesis of nanoparticles: concept, controversy and application. Nanoscale Res Lett 9:229

Hutchings GJ, Haruta M (2005) A golden age of catalysis: a perspective. Appl Catal A 291:2–5

Iqbal M, Ahmad A, Siddiqi TO (2011) Characterization of controversial plant drugs and effect of changing environment on active ingredients. In: Ahmad A, Siddiqi TO, Iqbal M (eds) Medicinal plants in changing environment. Capital Publishing Company, New Delhi, pp 1–10

Iqbal M, Ahmad A, Ansari MKA, Qureshi MI, Aref IM, Khan PR, Hegazy SS, El-Atta H, Husen A, Hakeem KR (2015) Improving the phytoextraction capacity of plants to scavenge metal(loid)-contaminated sites. Environ Rev 23:1–22

Iqbal M, Parveen R, Parveen A, Parveen B, Aref IM (2018) Establishing the botanical identity of plant drugs based on their active ingredients under diverse growth conditions. J Environ Biol 39(1):123–136

Islam NU, Jalil K, Shahid M, Muhammad N, Rauf A (2015a) *Pistacia integerrima* gall extract mediated green synthesis of gold nanoparticles and their biological activities. Arab J Chem. https://doi.org/10.1016/j.arabjc.2015.02.014

Islam NU, Jalil K, Shahid M, Rauf A, Muhammad N, Khan A, Raza Shah MR, Khan MA (2015b) Green synthesis and biological activities of gold nanoparticles functionalized with *Salix alba*. Arab J Chem. https://doi.org/10.1016/j.arabjc.2015.06.025

Jain A, Sinilal B, Starnes DL, Sanagala R, Krishnamurthy S, Sahi SV (2014) Role of Fe-responsive genes in bioreduction and transport of ionic gold to roots of Arabidopsis thaliana during synthesis of gold nanoparticles. Plant Physiol Biochem 84:189–196

Jayaseelan C, Ramkumar R, Rahuman AA, Perumal P (2013) Green synthesis of gold nanoparticles using seed aqueous extract of *Abelmoschus esculentus* and its antifungal activity. Ind Crop Prod 45:423–429

Joseph S, Mathew B (2015a) Microwave assisted facile green synthesis of silver and gold nanocatalysts using the leaf extract of *Aerva lanata*. Spectrochim Acta A Mol Biomol Spectrosc 136:1371–1379

Joseph S, Mathew B (2015b) Microwave-assisted green synthesis of silver nanoparticles and the study on catalytic activity in the degradation of dyes. J Mol Liq 204:184–191

Judy JD, Unrine JM, Rao W, Wirick S, Bertsch PM (2012) Bioavailability of gold nanomaterials to plants: importance of particle size and surface coating. Environ Sci Technol 46:8467–8474

Kasthuri J, Kathiravan K, Rajendiran N (2009) Phyllanthin assisted biosynthesis of silver and gold nanoparticles: a novel biological approach. J Nanopart Res 11:1075–1085

Khalil MMH, Ismail EH, Magdoub FE (2012) Biosynthesis of Au nanoparticles using *olive leaf* extract. Arab J Chem 5:431–437

Kneipp K, Haka AS, Kneipp H, Badizadegan K, Yoshizawa N, Boone C, Shafer-Peltier KE, Motz JT, Dasari RR, Feld MS (2002) Surface-enhanced Raman spectroscopy in single living cells using gold nanoparticles. Appl Spectrosc 56:150–154

Koo Y, Lukianova-Hleb EY, Pan J, Thompson SM, Lapotko DO, Braam J (2016) In planta response of *Arabidopsis* to photothermal impact mediated by gold nanoparticles. Small 12:623–630

Krishnaraj C, Muthukumaran P, Ramachandran R, Balakumaran MD, Kalaichelvan PT (2014) *Acalypha indica* Linn: biogenic synthesis of silver and gold nanoparticles and their cytotoxic effects against MDA-MB-231, human breast cancer cells. Biotechnol Rep 4:42–49

Kumar V, Yadav SK (2009) Plant-mediated synthesis of silver and gold nanoparticles and their applications. J Chem Technol Biotechnol 84:151–157

Kumar KP, Paul W, Sharma CP (2011) Green synthesis of gold nanoparticles with Zingiber officinale extract: characterization and blood compatibility. Process Biochem 46:2007–2013

Kumar KM, Mandal BK, Sinha M, Krishnakumar V (2012) *Terminalia chebula* mediated green and rapid synthesis of gold nanoparticles. Spectrochim Acta A Mol Biomol Spectrosc 86:490–494

Kumar V, Guleria P, Kumar V, Yadav SK (2013) Gold nanoparticle exposure induces growth and yield enhancement in Arabidopsis thaliana. Sci Total Environ 461–462:462–468

Kundu S, Panigrahi S, Praharaj S, Basu S, Ghosh SK, Pal A, Pal T (2007) Anisotropic growth of gold clusters to gold nanocubes under UV irradiation. Nanotechnology 18:075712

Kundu S, Lau S, Liang H (2009) Shape-controlled catalysis by cetyltrimethylammonium bromide terminated gold nanospheres, nanorods, and nanoprisms. J Phys Chem C 113:5150–5156

Kuppusamy P, Yusoff MM, Ichwan SJA, Parine NR, Maniam GP, Govindan N (2015) *Commelina nudiflora* L. edible weed as a novel source for gold nanoparticles synthesis and studies on different physical–chemical and biological properties. J Ind Eng Chem 27:59–67

Leu JG, Chen SA, Chen HM, Wu WM, Hung CF, Yao YD, Tu CS, Liang YJ (2012) The effects of gold nanoparticles in wound healing with antioxidant epigallocatechin gallate and α-lipoic acid. Nanomedicine 8:767–775

Li X, Robinson SM, Gupta A, Saha K, Jiang Z, Moyano DF, Sahar A, Riley MA, Rotello VM (2014) Functional gold nanoparticles as potent antimicrobial agents against multi-drug-resistant bacteria. ACS Nano 8:10682–10686

Lim SH, Ahn EY, Park Y (2016) Green synthesis and catalytic activity of gold nanoparticles synthesized by *Artemisia capillaris* water extract. Nanoscale Res Lett 11:474–484

Lin L, Wang W, Huang J, Li Q, Sun D, Yang X, Wang H, He N, Wang Y (2010) Nature factory of silver nanowires: plant mediated synthesis using broth of *Cassia fistula* leaf. Chem Eng J 162:852–858

Lisha KP, Pradeep T (2009) Enhanced visual detection of pesticides using gold nanoparticles. J Environ Sci Health B 44:697–705

Liu J, Lu Y (2003) A colorimetric lead biosensor using DNAzyme-directed assembly of gold nanoparticles. J Am Chem Soc 125:6642–6643

Lowery AR, Gobin AM, Day ES, Halas NJ, West JL (2006) Immuno nano shells for targeted photothermal ablation of tumor cells. Int J Nanomedicine 1:149–154

Lukman AI, Gong B, Marjo CE, Roessner U, Harris AT (2011) Facile synthesis, stabilization, and anti-bacterial performance of discrete ag nanoparticles using Medicago sativa seed exudates. J Colloid Interface Sci 353:433–444

Luo XL, Xu JJ, Du Y, Chen HY (2004) A glucose biosensor based on chitosan–glucose oxidase–gold nanoparticles biocomposite formed by one-step electrodeposition. Anal Biochem 334:284–289

Majumdar R, Bag BG, Maity N (2013) *Acacia nilotica* (Babool) leaf extract mediated size-controlled rapid synthesis of gold nanoparticles and study of its catalytic activity. Int Nano Lett 3:53–58

Manjari G, Saran S, Arun T, Devipriya SP, Rao AVB (2017) Facile *Aglaia elaeagnoidea* mediated synthesis of silver and gold nanoparticles: antioxidant and catalysis properties. J Clust Sci 28:2041–2056

Manju S, Malaikozhundan B, Vijayakumar S, Shanthi S, Jaishabanu A, Ekambaram P, Vaseeharan B (2016) Antibacterial, antibiofilm and cytotoxic effects of *Nigella sativa* essential oil coated gold nanoparticles. Microb Pathog 91:129–135

Medhe S, Bansal P, Srivastava MM (2014) Enhanced antioxidant activity of gold nanoparticle embedded 3,6-dihydroxyflavone: a combinational study. Appl Nanosci 4:153–161

Meyre ME, Tréguer-Delapierre M, Faure C (2008) Radiation induced synthesis of gold nanoparticles within lamellar phases. Formation of aligned colloidal gold by radiolysis. Langmuir 24:4421–4425

Mishra AN, Bhadauria S, Gaur MS, Pasricha R, Kushwah BS (2010) Synthesis of gold nanoparticles by leaves of zero-calorie sweetener herb (*Stevia rebaudiana*) and their nanoscopic characterization by spectroscopy and microscopy. Int J Green Nanotechnol Phys Chem 1:118–124

Mishra P, Ray S, Sinha S, Das B, Khan MI, Behera SK, Il Yun S, Tripathy SK, Mishra A (2016) Facile bio-synthesis of gold nanoparticles by using extract of *Hibiscus sabdariffa* and evaluation of its cytotoxicity against U87 glioblastoma cells under hyperglycemic condition. Biochem Eng J 105:264–272

Moaveni P, Karimi K, Valojerdi MZ (2011) The nanoparticles in plants. J Nano Struct Chem 2:59–78

Mock JJ, Barbic M, Smith DR, Schultz DA, Schultz S (2002) Shape effects in plasmon resonance of individual colloidal silver nanoparticles. J Chem Phys 116:6755–6759

Mollick MMR, Bhowmick B, Mondal D, Maity D, Rana D, Dash SK, Chattopadhyay S, Roy S, Sarkar J, Acharya K, Chakrabortye M, Chattopadhyay D (2014) Anticancer (in vitro) and antimicrobial effect of gold nanoparticles synthesized using *Abelmoschus esculentus* (L.) pulp extract via a green route. RSC Adv 4:37838–37849

Mukherjee P, Bhattacharya R, Bone N, Lee YK, Patra C, Wang S, Lu L, Secreto C, Banerjee PC, Yaszemski MJ, Kay NE, Mukhopadhyay D (2007) Potential therapeutic application of gold nanoparticles in B-chronic lymphocytic leukemia (BCLL): enhancing apoptosis. J Nanobiotechnol 5:4

Nair AS, Tom RT, Pradeep T (2003) Detection and extraction of endosulfan by metal nanoparticles. J Environ Monit 5:363–365

Narayanan KB, Sakthivel N (2008) *Coriander leaf* mediated biosynthesis of gold nanoparticles. Mater Lett 62:4588–4590

Narayanan KB, Sakthivel N (2010a) Biological synthesis of metal nanoparticles by microbes. Adv Colloid Interf Sci 156:1–13

Narayanan KD, Sakthivel N (2010b) Phytosynthesis of gold nanoparticles using leaf extract of *Coleus amboinicus Lour*. Mater Charact 61:1232–1238

Nellore J, Paulineb PC, Amarnathc K (2012) Biogenic synthesis by S*phearanthus Amaranthoids;* towards the efficient production of the biocompatible gold nanoparticles. Dig J Nanomater Biostruct 7:123–133

Neng J, Harpster MH, Zhang H, Mecham JO, Wilson WC, Johnson PA (2010) A versatile SERS-based immunoassay for immunoglobulin detection using antigen-coated gold nanoparticles and malachite green-conjugated protein A/G. Biosens Bioelectron 26:1009–1015

Noruzi M, Zare D, Khoshnevisan K, Davoodi D (2011) Rapid green synthesis of gold nanoparticles using *Rosa hybrida* petal extract at room temperature. Spectrochim Acta A Mol Biomol Spectrosc 79:1461–1465

Nun YS, Jaroenrama W, Sriurairatana S, Suebsing R, Kiatpathomchai W (2013) Visual detection of white spot syndrome virus using DNA-functionalized gold nanoparticles as probes combined with loop-mediated isothermal amplification. Mol Cell Probes 27:71–79

Okitsu K, Mizukoshi Y, Yamamoto TA, Maeda Y, Nagata Y (2007) Sonochemical synthesis of gold nanoparticles on chitosan. Mater Lett 61:3429–3431

Orendorff CJ, Gole A, Sau TK, Murphy CJ (2005) Surface enhanced Raman spectroscopy of self-assembled monolayers: Sandwich architecture and nanoparticle shape dependence. Anal Chem 77:3261–3266

Ovais M, Raza A, Naz S, Islam NU, Khalil AT, Ali S, Khan MA, Shinwari ZA (2017) Current state and prospects of the phytosynthesized colloidal gold nanoparticles and their applications in cancer theranostics. Appl Microbiol Biotechnol 101:3551–3565

Pandey S, Oza G, Mewada A, Madhuri S (2012) Green synthesis of highly stable gold nanoparticles using *Momordica charantia* as Nano fabricator. Arch Appl Sci Res 4:1135–1141

Pasca RD, Mocanu A, Cobzac SC, Petean I, Horovitz O, Tomoaia-Cotisel M (2014) Biogenic syntheses of gold nanoparticles using plant extracts. Part Sci Technol 32:131–137

Peleg G, Lewis A, Linial M, Loew LM (1999) Nonlinear optical measurement of membrane potential around single molecules at selected cellular sites. Proc Natl Acad Sci U S A 96:6700–6704

Phillip D (2009) Biosynthesis of Ag, Au and Au-Ag nanoparticles using edible mushrooms extracts. Spectrochim Acta A Mol Biomol Spectrosc 73:374–381

Philip D (2010) Rapid green synthesis of spherical gold nanoparticles using *Mangifera indica* leaf. Spectro Acta A Mol Biomol Spectrosc 77:807–810

Philip D, Unnib C, Aromala SA, Vidhua VK (2011) Murraya Koenigii leaf-assisted rapid green synthesis of silver and gold nanoparticles. Spectrochim Acta A Mol Biomol Spectrosc 78:899–904

Piruthiviraj P, Margret A, Krishnamurthy PP (2016) Gold nanoparticles synthesized by *Brassica oleracea* (Broccoli) acting as antimicrobial agents against human pathogenic bacteria and fungi. Appl Nanosci 6:467–473

Pradeep T, Anshup A (2009) Noble metal nanoparticles for water purification: a critical review. Thin Solid Films 517:6441–6478

Qian XM, Nie S (2008) Single-molecule and single-nanoparticle SERS: from fundamental mechanisms to biomedical applications. Chem Soc Rev 37:912–920

Ramachandran R, Krishnaraj C, Sivakumar AS, Prasannakumar P, Kumar VKA, Shim KS, Song CG, Yun SII (2017) Anticancer activity of biologically synthesized silver and gold nanoparticles on mouse myoblast cancer cells and their toxicity against embryonic zebrafish. Mater Sci Eng C 73:674–683

Ramakrishna M, Babu DR, Gengan RM, Chandra S, Rao GN (2016) Green synthesis of gold nanoparticles using marine algae and evaluation of their catalytic activity. J Nanostructure Chem 6:1–13

Rana S, Bajaj A, Mout R, Rotello VM (2012) Monolayer coated gold nanoparticles for delivery applications. Adv Drug Deliv Rev 64:200–216

Rao KJ, Paria S (2014) Green synthesis of gold nanoparticles using aqueous *Aegle marmelos* leaf extract and their application for thiamine detection. RSC Adv 4:28645–28652

Raouf NA, Al-Enazib NM, Ibraheem IBM (2017) Green biosynthesis of gold nanoparticles using *Galaxaura elongata* and characterization of their antibacterial activity. Arab J Chem 10:S3029–S3039

Reddy V, Torati RS, Oh S, Kim C (2012) Biosynthesis of gold nanoparticles assisted by *Sapindus mukorossi* gaertn. Fruit pericarp and their catalytic application for the reduction of *p*-nitroaniline. Ind Eng Chem Res 52:556–564

Sadeghi B, Mohammadzadeh M, Babakhani B (2015) Green synthesis of gold nanoparticles using *Stevia rebaudiana* leaf extracts: characterization and their stability. J Photochem Photobiol B 148:101–106

Sathish KG, Jha PK, Vignesh V, Rajkuberan C, Jeyaraj M, Selvakumar M, Jha R, Sivaramakrishnan S (2016) Cannonball fruit (*Couroupita guianensis*, Aubl.) extract mediated synthesis of gold nanoparticles and evaluation of its antioxidant activity. J Mol Liq 215:229–236

Sett A, Gadewar M, Sharma P, Deka M, Bora U (2016) Green synthesis of gold nanoparticles using aqueous extract of *Dillenia indica*. Adv Nat Sci Nanosci Nanotechnol 7:025005–025013

Shaligram NS, Bule M, Bhambure R, Singhal RS, Singh SK, Szakacs G, Pandey A (2009) Biosynthesis of silver nanoparticles using aqueous extract from the compactin producing fungal strain. Process Biochem 44:939–943

Shankar SS, Ahmad A, Pasricha R, Sastry M (2003) Bioreduction of chloroaurate ions by geranium leaves and its endophytic fungus yields gold nanoparticles of different shapes. J Mater Chem 13:1822–1826

Shankar SS, Rai A, Ankamwar B, Singh A, Ahmad A, Sastry M (2004) Biological synthesis of triangular gold Nanoprisms. Nat Mater 3:482–488

Shankar SS, Rai A, Ahmad A, Sastry M (2005) Controlling the optical properties of lemongrass extract synthesized gold nanotriangles and potential application in infrared-absorbing optical coatings. Chem Mater 17:566–572

Sharma NC, Sahi SV, Nath S, Parsons JG, Gardea-Torresdey JL, Tarasankar P (2007) Synthesis of plant-mediated gold nanoparticles and catalytic role of biomatrix-embedded nanomaterials. Environ Sci Technol 41:5137–5142

Siddiqi KS, Husen A (2016) Engineered gold nanoparticles and plant adaptation potential. Nanoscale Res Lett 11:400

Siddiqi KS, Husen A (2017a) Recent advances in plant-mediated engineered gold nanoparticles and their application in biological system. J Trace Elem Med Biol 40:10–23

Siddiqi KS, Husen A (2017b) Plant response to engineered metal oxide nanoparticles. Nanoscale Res Lett 12:92

Siddiqi KS, Rahman A, Tajuddin HA (2016) Biogenic fabrication of iron/iron oxide nanoparticles and their application. Nanoscale Res Lett 11:498

Siddiqi KS, Husen A, Rao RAK (2018a) A review on biosynthesis of silver nanoparticles and their biocidal properties. J Nanobiotechnol 16:14

Siddiqi KS, Rahman A, Tajuddin, Husen A (2018b) Properties of zinc oxide nanoparticles and their activity against microbes. Nanoscale Res Lett 13:141

Siddiqi KS, Husen A, Sohrab SS, Osman M (2018c) Recent status of nanomaterials fabrication and their potential applications in neurological disease management. Nanoscale Res Lett 13:231

Siddiqi KS, Rashid M, Rahman A, Tajuddin, Husen A, Rehman S (2018d) Biogenic fabrication and characterization of silver nanoparticles using aqueous-ethanolic extract of lichen (*Usnea longissima*) and their antimicrobial activity. Biomat Res 22:23

Singh AK, Srivastava ON (2015) One-step green synthesis of gold nanoparticles using black cardamom and effect of pH on its synthesis. Nanoscale Res Lett 10:353–364

Smitha SL, Philip D, Gopchandran KG (2009) Green synthesis of gold nanoparticles using *Cinnamomum zeylanicum* leaf broth. Spectrochim Acta A Mol Biomol Spectrosc 74:735–739

Song JY, Jang H-K, Kim BS (2009) Biological synthesis of gold nanoparticles using *Magnolia kobus* and *Diospyros kaki* leaf extracts. Process Biochem 44:1133–1138

Sreelakshmi C, Datta K, Yadav J, Reddy B (2011) Honey derivatized Au and Ag nanoparticles and evaluation of its antimicrobial activity. J Nanosci Nanotechnol 11:6995–7000

Suganthy N, Ramkumar VS, Pugazhendhi A, Benelli G, Archunan G (2018) Biogenic synthesis of gold nanoparticles from *Terminalia arjuna* bark extract: assessment of safety aspects and neuroprotective potential via antioxidant, anticholinesterase, and antiamyloidogenic effects. Environ Sci Pollut Res 25:10418–10433

Suman TY, Rajasree SRR, Ramkumar R, Rajthilak C, Perumal P (2014) The Green synthesis of gold nanoparticles using an aqueous root extract of *Morinda citrifolia* L. Spectrochim Acta A Mol Biomol Spectrosc 118:11–16

Suvith VS, Philip D (2014) Catalytic degradation of methylene blue using biosynthesized gold and silver nanoparticles. Spectrochim Acta A Mol Biomol Spectrosc 118:526–532

Thanh NTK, Rosenzweig Z (2002) Development of an aggregation-based immunoassay for anti-protein a using gold nanoparticles. Anal Chem 74:1624–1628

Tiloke C, Phulukdaree A, Anand K, Gengan RM, Chuturgoon AA (2016) *Moringa oleifera* gold nanoparticles modulate oncogenes, tumor suppressor genes, and caspase-9 splice variants in A549 cells. J Cell Biochem 117:2302–2314

Tsuji T, Kakita T, Tsuji M (2003) Preparation of nano-size particles of silver with femtosecond laser ablation in water. Appl Surf Sci 206:314–320

Upadhyay P, Hanif M, Bhaskar S (2006) Visual detection of IS6110 of Mycobacterium tuberculosis in sputum samples using a test based on colloidal gold and latex beads. Clin Microbiol Infect 12:1118–1122

Vankar PS, Bajpai D (2010) Preparation of gold nanoparticles from Mirabilis jalapa flowers. Ind J Biochem Biophys 47:157–160

Vance ME, Kuiken T, Vejerano EP, McGinnis SP, Hochella MF Jr, Rejeski D, Hull MS (2015) Nanotechnology in the real world: redeveloping the nanomaterial consumer products inventory. Beilstein J Nanotechnol 6: 1769–1780

Velammal SP, Devi TA, Amaladhas TP (2016) Antioxidant, antimicrobial and cytotoxic activities of silver and gold nanoparticles synthesized using *Plumbago zeylanica* bark. J Nanostruct Chem 6:247–260

Vijayakumar S, Vaseeharan B, Malaikozhundan B, Gopi N, Ekambaram P, Pachaiappan R, Velusamy P, Murugan K, Benelli G, Kumar RS, Suriyanarayanamoorthy M (2017) Therapeutic effects of gold nanoparticles synthesized using *Musa paradisiaca* peel extract against multiple antibiotic resistant Enterococcus faecalis biofilms and human lung cancer cells (A549). Microb Pathog 102:173–183

Vijayaraghavan K, Nalini SPK (2010) Biotemplates in the green synthesis of silver nanoparticles. Biotechnol J 5:1098–1110

Wang R, Yue L, Yu Y, Zou X, Song D, Liu K, Liu Y, Su H (2016) Gold nanoparticles modify the photophysical and photochemical properties of 6-thioguanine: preventing DNA oxidative damage. J Phys Chem C 120:14410–14415

Watters JL, Satia JA, Kupper LL, Swenberg JA, Schroeder JC, Switzer BR (2007) Associations of antioxidant nutrients and oxidative DNA damage in healthy African-American and white adults. Cancer Epidemiol Biomark Prev 16:1428–1436

Wilson-Corral V, Anderson CWN, Rodriguez-Lopez M (2012) Gold phytomining. A review of the relevance of this technology to mineral extraction in the 21st century. J Environ Manag 111:249–257

Yasmin A, Ramesh K, Rajeshkumar S (2014) Optimization and stabilization of gold nanoparticles by using herbal plant extract with microwave heating. Nano Converg 1:12

Yu J, Xu D, Guan HN, Wang C, Huang LK, Chi DF (2016) Facile one-step green synthesis of gold nanoparticles using *Citrus maxima* aqueous extracts and its catalytic activity. Mater Lett 166:110–112

Zamarion VM, Timm RA, Araki K, Toma HE (2008) Ultrasensitive SERS nanoprobes for hazardous metal ions based on trimercaptotriazine-modified gold nanoparticles. Inorg Chem 47:2934–2936

Zhan G, Huang J, Lin L, Lin W, Emmanuel K, Li Q (2011) Synthesis of gold nanoparticles by *Cacumen Platycladi* leaf extract and its simulated solution: toward the plant-mediated biosynthetic mechanism. J Nanopart Res 13:4957–4968